PHILOSOPHICAL TRANSACTIONS OF THE ROYAL SOCIETY A MATHEMATICAL, PHYSICAL & ENGINEERING SCIENCES

Effective conductivity of loaded granular materials by numerical simulation

Alexander Z. Zinchenko

Phil. Trans. R. Soc. Lond. A 1998 **356**, 2953-2998
doi: 10.1098/rsta.1998.0305

THE ROYAL SOCIETY

Effective conductivity of loaded granular materials by numerical simulation

By Alexander Z. Zinchenko

Department of Chemical Engineering, University of Colorado, Boulder, CO 80309-0424, USA

Received 31 January 1996; revised 17 November 1996; accepted 10 June 1997

Contents

1. Introduction 2954
2. Local flux between two touching highly conducting spheres 2958
   (*a*) The case of point contacts 2958
   (*b*) Two spheres with a small contact spot 2962
3. Matched asymptotic expansion strategy for conductivity simulations 2966
4. Random close packings and the calculation of contact deformations 2970
5. Solution of the boundary-value problem 2975
6. Numerical results 2980
7. Comparison with experiments 2990
8. Conclusions and future work 2992
Appendix A. The analysis of a model two-sphere problem 2993
Appendix B. The expansion of a harmonic function into spherical harmonics 2994
Appendix C. An absolutely stable scheme for calculating Wigner functions 2995
References 2996

Thermal (or electrical) conduction through a stationary, random close-packed granular material is studied by numerical simulation. The particles are smooth uniform spheres with either point contacts, or small contact spots under a mechanical load (resulting in practice from the transmitted bed weight or applied pressure), and the particle-to-medium conductivity ratio, γ, is assumed to be high (typically, up to $O(10^3)$). To simulate particle arrangements, a recent random close-packing algorithm for $N \gg 1$ absolutely rigid spheres in a periodic box is used, and small contact deformations are rigorously calculated as a perturbation from the Hertz theory and a mechanical balance of normal contact reactions on the microscale. To solve the conduction boundary-value problem for $N \gg 1$ and $\gamma \gg 1$, when all the existing 'exact' simulation techniques lead to prohibitive convergence difficulties, a novel, asymptotic algorithm is developed and shown to be highly accurate for all $\gamma \geqslant 100$. This algorithm is based on matching the outer solution for perfectly conducting spheres in point contact with the near-contact solutions (that include the effects of finite γ and small deformation), to provide additional equations for unknown particle temperatures (or potentials) in the outer geometry. The outer problem is then 'regularized' and solved by a special economical multipole method. Using these techniques for $N \leqslant 200$ and configurational averaging, the non-dimensional effective conductivity f^* is found as a universal function of γ and $\Pi = [\langle p \rangle (1-\nu^2)/E]^{1/3}$, where $\langle p \rangle$ is

the average pressure in the material, and ν and E are the particle Poisson ratio and Young's modulus. These results are complemented by the exact values of $f^*(\gamma)$ for a material with point contacts and $\gamma < 100$. Conduction through a random close packing of nearly rigid spheres in a vacuum environment is also considered.

Keywords: effective conductivity; granular materials; random close packing; disordered materials; multipole methods; multiparticle interaction

1. Introduction

Transport properties of granular materials, such as the effective thermal or electrical conductivity, are important in thermal insulation, powder technology, cryogenic systems, and many other applications. It is particularly useful to know, from first principles, how the method of preparation of a granular material and its microstructure affect the bulk properties. The characteristic features of a stationary random granular material are (i) an equilibrium mechanical contact network formed by inclusions and (ii) a typically very high ratio $\gamma = \Lambda'/\Lambda^{\mathrm{e}} = O(10^2\text{–}10^3)$ of particle-to-medium conductivities. Compared to a simpler case of suspensions, where considerable theoretical progress has been made, relatively little work was reported on calculating the effective transport properties of granular materials from their microstructure. In pioneering research, Batchelor & O'Brien (1977) considered a random packed bed of monodisperse spheres with $\gamma \gg 1$, when the conduction is mainly through near-contact areas, and found the effective conductivity to be $\Lambda^* \sim 4.0\Lambda^{\mathrm{e}} \ln\gamma$. Due to a weak, logarithmic singularity, the local fluxes through the near-contact regions are not quite dominant for practically interesting γ and, instead of considering a more difficult outer problem, Batchelor & O'Brien adjusted their result to experimental data, to obtain $\Lambda^*/\Lambda^{\mathrm{e}} \approx 4.0\ln\gamma - 11$. This relation, however, is subject to some uncertainty. First, the factor 4.0 is a result of an approximate, analytical averaging, with an unknown error, and based on a somewhat arbitrary proximity criterion to find the average coordination number (i.e. the number of contacts per particle) from experimental data. Second, the conductivity measurements are widely scattered, which can make the empirical constant of -11 unreliable. It would be practically useful to include additional physical factors, responsible for this scatter, in the theoretical calculations, rather than consider the dimensionless conductivity $f^* = \Lambda^*/\Lambda^{\mathrm{e}}$ as a unique function of γ. One of the most important factors is the contact deformation. In a free-standing bed subject to gravity, particles transmit weight and form small contact spots, rather than point contacts, which can substantially increase the effective conductivity, if $\gamma \gg 1$; this effect can be further amplified by applying an additional load to a bed. Using a boundary-integral analysis and the solution of the Hertz contact problem, Batchelor & O'Brien showed that, when two spheres of radius a are pressed together to form a small contact spot of radius ρ, the local flux is considerably enhanced if $\gamma\rho/a \geqslant O(10)$. However, we are not aware of any theoretical calculations of the effective conductivity for deformable particles, as a further development of this idea (apart from the work of Chan & Tien (1973), who considered the simplest and very restrictive case of regular packings in a vacuum environment, when the conduction is only through the contact spots).

In the present paper, which is a considerable extension of Batchelor & O'Brien's analysis and was largely motivated by their pioneering study, a novel, rigorous, and

highly accurate mathematical approach to calculating the effective conductivity of granular materials is developed based on numerical simulation. The problem is solved in the classical, somewhat idealized formulation, for smooth monodisperse spheres in an isotropic *random close packing*, with either point contacts, or small contact spots under a mechanical load. Realistic frictional particles, having been poured into a large vessel, normally produce a packing between the limits of random 'loose' and close packings and shrink to the close packing only after a subsequent bed shaking or vibration (Scott & Kilgour 1969). We focus on the random close packing, since it is a statistically reproducible state, independent of the interparticle friction (Scott & Kilgour 1969), and put aside friction effects for further investigation. The contact spot radii and near-contact deformations are rigorously calculated from the Hertz theory and the mechanical balance of contact forces on the microscale, given the average pressure in the material as a macroscopic parameter. In the effective conductivity calculations, perfect contacts are assumed. One can argue that the inevitable surface roughness in the contact areas is important, and, indeed, there have been numerous experimental and semi-empirical studies of contact resistance phenomena (Song & Yovanovich 1988; Song *et al*. 1989, 1993; Negus *et al*. 1987; McWaid & Marshall 1992; Sridhar & Yovanovich 1994, and other works). However, all the experiments have been made for nominally flat surfaces, at apparent contact pressures not exceeding 12 MPa. In static granular materials, the contact pressures are typically much higher, due to the very small contact areas. For a free-standing bed, e.g. the apparent interparticle contact pressure P at a depth z can be estimated from the Hertzian contact area (Landau & Lifshitz 1959) and the macroscopic force balance as

$$P \sim 0.5\left[\Delta\rho g z\left(\frac{E}{1-\nu^2}\right)^2\right]^{1/3},$$

where $\Delta\rho$ is the density difference between the particles and the medium, g is the gravity acceleration, E and ν are the particle Young's modulus and the Poisson ratio. For steel spheres in a gas environment, this estimate yields relatively large values of $P \sim 170$–630 MPa for $z = 1$–50 cm. Obviously, the existing correlations for the contact resistance, all semi-empirical, cannot be relied upon far outside the range of pressures where they were fitted to experimental data. On the other hand, experimental measurements of the contact heat transfer between a steel bearing ball of several millimetres in size and a wall at contact pressures of about 1600 MPa were found to be in excellent agreement with calculations, based on the Hertzian theory and the assumption of perfect thermal contact (Nakajima 1995). At present, one can only speculate about the effect of asperities on the granular media conductivity, and we neglect this effect (as well as the possible presence of superficial oxide layers). When available, relevant contact resistance data at high pressures can easily be included in our simulation method, as discussed in § 7. Note that the plastic deformations of individual asperities do not preclude from using the Hertzian theory at length-scales exceeding the asperity size. Indeed, the normal load compliance for granular particles was found to be in very good agreement with the Hertzian theory (Mullier *et al*. 1991). At the same time, for tangential loads, when the role of asperities is crucial, the experiments of Mullier *et al*. (1991) question the validity of the Mindlin–Deresiewicz (Mindlin & Deresiewicz 1953) theory, developed for elastic contacts, which is one more reason to leave aside tangential effects at the present stage of our work.

Our approach to the conductivity simulations takes the deformation as a small, but singular perturbation and requires (i) an adequate packing algorithm to prepare an isotropic, mechanically equilibrium contact network of $N \gg 1$ *non-deformed* spheres in a cell with triply periodic boundaries and (ii) a method to solve the conduction multiparticle boundary-value problem for $\gamma \gg 1$ (including the whole practically interesting range of $\gamma \geqslant O(10^2)$), with allowance for contact deformations. Without periodic boundaries, it would be practically impossible to attain the limit $N \to \infty$ in the conductivity simulations.

Early packing methods with periodic boundaries, both purely geometrical (Jodrey & Tory 1981, 1985; Moscinski *et al*. 1989) and 'thermodynamic', based on molecular dynamics or Monte-Carlo-like densification procedures (e.g. Woodcock 1976), are all *kinetics-determined*, i.e. they contain the densification rate as an arbitrary parameter; discouragingly, sufficiently slow densification leads to complete or partial crystallization, as discussed by Zinchenko (1994*b*). The inadequacy of these methods for simulating a packing of a granular material is also due to the fact that they were not aimed at preparing a mechanically equilibrium network. On the other hand, in granular media mechanics, there have been a large number of works using a dynamic, discrete element method (e.g. Cundall & Strack 1979; Zhang & Cundall 1986; Barbosa & Ghaboussi 1990, 1992; Dobry & Ng 1992 and numerous references therein); recently, a quasi-static approach, which is more efficient for equilibrium problems, has been developed (Goddard *et al*. 1993, 1994; Bagi 1993; Bojtár & Bagi 1993). In these methods, particles are assumed to have some compliance, and different contact laws are used. Although this approach is very general and has a clear mechanical sense, none of these works claimed to have solved a particular problem of random close packing; the computations for 'nearly rigid' spheres are obviously very difficult because of the numerical stiffness.

In the present work, we use a recent packing algorithm of Zinchenko (1994*b*) for *absolutely rigid* spheres. In this algorithm, at the main stage of densification, particles swell while keeping the existing contacts (to avoid crystallization), until a new contact occurs and one of the existing bonds is broken to continue the densification, and so on. Most importantly, this purely geometric algorithm terminates when the spheres reach a mechanical equilibrium under the action of normal contact reactions, and results in a perfect contact network with the average coordination number of six. To the best of our knowledge, this, *kinetics-independent* algorithm is the only one that has demonstrated an unambiguous convergence, as $N \to \infty$, to the experimental random close-packing density (about 0.637); besides, close agreement of the theoretical and experimental microstructures (Zinchenko 1994*b*) validates the hypothesis that the gravitational random close packings, far from the boundaries, can be accurately modelled as isotropic. Although this algorithm is quite successful in simulating random close packings, we should note, however, that in future conductivity calculations for friction–determined beds, the packing method of Goddard *et al*. (1993, 1994), or similar methods for 'nearly rigid' spheres, may have no alternative.

As for the solution of the multiparticle boundary-value problems, there have been generally successful conductivity simulations for concentrated suspensions of spheres, using multipole expansions (Sangani & Yao 1988), a random walker method (Kim & Torquato 1991) and an approximate Stokesian dynamics-like approach (Bonnecaze & Brady 1990, 1991). A unique feature of the random-walker method is its applicability, in principle, to an arbitrary microstructure, which was demonstrated by the

conductivity simulations for random dispersions of aligned spheroids and of freely overlapping spheres (Kim & Torquato 1992, 1993). Granular materials, however, present a very difficult case, even for $\gamma \sim 10^2$ (let alone more interesting values $\gamma \sim 10^3$). Indeed, the conductivity in this case is sensitive to the details of the solution in the near-contact regions and, to attain a reasonable accuracy, a walker should spend considerable 'time' there, both inside and outside the inclusions. Instead, a random-walker is trapped in a single inclusion, with a very small probability $p_1 \sim 1/\gamma$ (Kim & Torquato 1991) of jumping into the interparticle space, once it has reached the interface. In the same case, the direct multipole method also meets severe convergence difficulties. The dipole and quadrupole formulations of the Stokesian dynamics approach were found to give considerably different results in the special case of highly concentrated random suspensions of superconducting spheres (Bonnecaze & Brady 1991, fig. 4a), and, from their comparison with the random-walker calculations of Kim & Torquato (1991), it is hard to decide which of the two approximations, dipole or quadrupole, would be better in the relevant case of random close packings with large, but finite γ. It is likely that, to remove this ambiguity and obtain good convergence, many more multipoles would be required, even with exact two-body interactions included, which is computationally very difficult for $N \gg 1$ using the Stokesian dynamics approach. For all the above reasons, granular materials, in contrast to suspensions, present a quite new simulation problem that requires a novel approach. Zinchenko (1994*a*) has newly developed a special, economical multipole technique to consider conduction through a multiparticle system of spheres at arbitrary γ. This method, with the convergence to the exact solution, is based on the idea that only the interaction of low-order harmonics is long-ranged to construct an 'economical truncation', and also uses rotational transformations of spherical harmonics by Wigner functions to considerably optimize the 'near-field' summations and effectively include multipoles of very high order, when necessary. This method is suitable for calculating the effective conductivities of relatively large random close packings with point contacts and small-to-moderately large γ (§ 6). However, when both γ and N are large, even this algorithm, orders-of-magnitude faster than traditional multipole techniques, becomes prohibitively expensive; besides, it does not include, in principle, the possibility of particle deformations, nor do the solutions of Sangani & Yao (1988) and Bonnecaze & Brady (1990, 1991). In the present work, we combine the most efficient elements of Zinchenko's algorithm with the method of matched asymptotic expansions to develop a novel, highly accurate *asymptotic* algorithm for $\gamma \gg 1$ and small contact deformations. The idea of considering deformation as a small, but singular perturbation and of using matched asymptotic expansions has proved fruitful in two-particle and two-drop problems (Davis *et al*. 1986; Yiantsios & Davis 1990, 1991). The present solution seems to be the first application of matched asymptotic expansions to a random multiparticle system.

The problems of determining effective transport coefficients (thermal or electrical conductivity, dielectric constant, magnetic permeability) are all mathematically equivalent, if we neglect specific mechanisms like thermal radiation (which is essential only at very high temperatures); for definiteness, thermal conduction is considered herein. In § 2 *a*, an expression for the local flux between two highly conducting spheres in point contact is derived. This problem was first studied numerically by Batchelor & O'Brien (1977), but we find a more attractive, analytical solution, capable of better accuracy. This solution (which may have additional applications) is used in the

boundary-integral calculations of § 2 *b*, to obtain a complete description of the local thermal flux between two particles with a small contact spot, in addition to a few numerical results of Batchelor & O'Brien. In § 3, a central part of the paper, a rigorous asymptotic strategy for the solution of the boundary-value problem is described. We neglect the $O(\gamma^{-1})$-corrections due to the particle temperature non-uniformity in the outer region, far from contacts, but take $\ln\gamma$ as a finite parameter (which is computationally very efficient), and so the outer particle temperatures are unknown and coupled to the near-contact solutions (§ 2) through matching. The outer multiparticle problem, for superconducting spheres at different temperatures in point contact, is well-posed, but singular, and cannot be solved by multipole techniques. We show, however, how to reduce this problem, with a very small error, to conduction through a system of non-touching superconducting spheres of slightly contracted radius with possible heat sources/sinks inside; original finite particle conductivity and elasticity are effectively accounted for in the 'heat-transfer coefficients' between neighbouring superconductors. This new problem is efficiently solved by Zinchenko's (1994*a*) economical multipole technique, with some new features (§ 5); making then the artificial gap ϵ arbitrarily small, we approach the solution of the initial, singular outer problem. It turns out that, to achieve high accuracy, ϵ does not have to be very small, and so our multipole expansions remain reasonably fast-converging. In § 4, we discuss Zinchenko's (1994*b*) packing algorithm and extend his calculations, to prepare random close packings with $N \leqslant 200$ and perfect contactness and also find contact deformations, as a perturbation. Conductivity calculations are presented in § 6. In the absence of deformations, a comparison is made with the exact, but computationally very intensive, calculations for several small to moderately large packings, with γ up to several hundred, to demonstrate a high accuracy of our asymptotic algorithm in the whole range $\gamma \geqslant 100$; it is also shown that an alternative approach, an expansion in inverse powers of $\ln\gamma$, would be very inefficient. For a granular material with contact deformations, for which there seems to be no prospect of exact results, the non-dimensional effective conductivity, $f^* = \Lambda^*/\Lambda^{\mathrm{e}}$, is calculated by the asymptotic algorithm as a universal function of γ and the elastic parameter $\Pi = [\langle p\rangle(1-\nu^2)/E]^{1/3}$ (with $\langle p\rangle$ being the average pressure in the material) in the whole range $\gamma = O(10^2$–$10^3)$ of practical interest, using $N \leqslant 200$ and configurational averaging. These calculations are complemented by the exact values of $f^*(\gamma)$ for a material with point contacts and $\gamma < 100$. The simplest case of conduction through a random close packing in 'vacuum environment' is also considered. The statistical and finite-size errors are analysed and found to be very small. In § 7, we comment on the relation of our theory to the experimental data.

The calculations have been performed mainly on an IBM AIX R/6000 workstation.

2. Local flux between two touching highly conducting spheres

(*a*) *The case of point contacts*

We are first interested in the expression for the local thermal flux between two touching, identical spherical particles with surfaces S_α and S_β, radius a, and high particle-to-medium conductivity ratio γ, to be used in our scheme of matched asymptotic expansions. The particle temperatures T_α and T_β, far from the contact point, considered uniform due to $\gamma \gg 1$, are assumed to be given. This local problem was first addressed in Batchelor & O'Brien (1977) by a boundary integral analysis. For

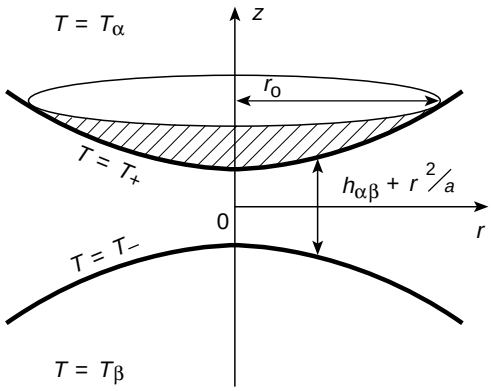

Figure 1. On the calculation of the local thermal flux between two nearly touching highly conducting spheres.

the purposes of the present work, their results are summarized briefly below, and a novel, *analytical* approach, capable of a higher accuracy, is developed.

It is convenient to consider first the case of slightly separated spheres, with a minimum gap thickness $h_{\alpha\beta} = \epsilon_{\alpha\beta}a$, and then take the limit $\epsilon_{\alpha\beta} \to 0$. Let (r, z) be a cylindrical coordinate system with the origin at the gap midpoint and (x, y) be Cartesian coordinates in the midplane $z = 0$ (figure 1). Locally, the heat conducted in a particle spreads out in an effectively semi-infinite medium, which allows boundary integral representations for the temperature distributions $T_+(x, y)$ and $T_-(x, y)$ on S_α and S_β, respectively, in the near-contact region, e.g.

$$T_+(x,y) = T_\alpha + \frac{1}{2\pi\gamma}\int_{-\infty}^{\infty}\int_{-\infty}^{\infty}\frac{1}{\{(x'-x)^2+(y'-y)^2\}^{1/2}}\frac{\partial T^{\mathrm{e}}}{\partial n}(x',y')\,\mathrm{d}x'\mathrm{d}y', \quad (2.1)$$

where $\partial T^{\mathrm{e}}/\partial n$ is the derivative on S_α in the direction of the outward normal $\boldsymbol{n}$, with the index e marking the values related to the continuous phase. This normal derivative can be approximated as $(T_- - T_+)/(h_{\alpha\beta} + r^2/a)$ from the assumption that the temperature varies approximately linearly across the gap. Using the symmetry properties,

$$T_+(x,y) - T_\alpha = T_\beta - T_-(x,y) = \tfrac{1}{2}(T_\beta - T_\alpha)f \quad (2.2)$$

yields the boundary integral equation for the function $f(x, y)$:

$$f(x,y) = \frac{1}{\pi\gamma}\int_{-\infty}^{\infty}\int_{-\infty}^{\infty}\frac{1-f(x',y')}{(h_{\alpha\beta}+r'^2/a)}\frac{\mathrm{d}x'\mathrm{d}y'}{\{(x-x')^2+(y'-y)^2\}^{1/2}}. \quad (2.3)$$

Since the solution is axisymmetric, (2.3) can be transformed to (Batchelor & O'Brien 1977)

$$f(\sigma) = \int_0^{\infty}\frac{1-f(\sigma')}{\lambda+\sigma'^2}I\left(\frac{\sigma'}{\sigma}\right)\mathrm{d}\sigma', \quad (2.4)$$

where

$$I\left(\frac{\sigma'}{\sigma}\right) = \frac{1}{\pi}\int_0^{2\pi}\frac{\sigma'\,\mathrm{d}\phi}{(\sigma'^2+\sigma^2-2\sigma\sigma'\cos\phi)^{1/2}} = \frac{4\sigma'}{\pi(\sigma+\sigma')}K\left(\frac{4\sigma'\sigma}{(\sigma'+\sigma)^2}\right), \quad (2.5)$$

K is the complete elliptic integral of the first kind, and the dimensionless quantities σ and λ are defined as

$$\sigma = \gamma r/a, \qquad \lambda = \gamma^2 \epsilon_{\alpha\beta}. \tag{2.6}$$

The heat flux

$$2\pi \Lambda^{\mathrm{e}}(T_\alpha - T_\beta) \int_0^{r_0} \frac{1-f}{h_{\alpha\beta} + r^2/a} r \, \mathrm{d}r \tag{2.7}$$

through a circular portion $D_{\alpha\beta}$ of S_α (shadowed in figure 1), with the cut-off radius r_0 in the region $a\epsilon_{\alpha\beta}^{1/2} \ll r_0 \ll a$ of overlapping with the outer solution (§ 3), can be written as

$$\pi \Lambda^{\mathrm{e}} a (T_\alpha - T_\beta)[\ln r_0^2/a^2 + \ln \epsilon_{\alpha\beta}^{-1} - P(\lambda) + o(1)], \tag{2.8}$$

where

$$P(\lambda) = \int_0^\infty \frac{2f(\sigma)\sigma \mathrm{d}\sigma}{\lambda + \sigma^2}. \tag{2.9}$$

The convergence of the integral (2.9) follows from the asymptotics (Batchelor & O'Brien 1977) $f(\sigma) \sim 2 \ln \sigma/\sigma$ at $\sigma \to \infty$.

Finally, the asymptotics of $P(\lambda)$ in the necessary limit $\lambda \to 0$ of touching spheres was found to be

$$P(\lambda) \sim \ln \lambda^{-1} + 3.9 + 0.1\lambda, \tag{2.10}$$

where the coefficients 3.9 and 0.1 were estimated by Batchelor & O'Brien from the numerical solution of (2.4) at $\lambda \ll 1$. The coefficient 3.9 is not accurate enough for the purposes of the present work (in particular, for the comparison of exact and asymptotic conductivity simulations undertaken in § 6), and the accuracy cannot be improved easily by the numerical solution of (2.4), because the integrals (2.4) and (2.9) are very slowly (and monotonically) convergent. Instead, we have found a surprisingly simple analytical solution, as described below.

Let ξ, η be bispherical coordinates defined as

$$z = \frac{c \sinh \eta}{\cosh \eta - \mu}, \qquad \rho = \frac{c \sin \xi}{\cosh \eta - \mu}, \qquad \mu = \cos \xi, \qquad 0 \leqslant \xi \leqslant \pi. \tag{2.11}$$

The spheres S_α and S_β become coordinate surfaces $\eta = \eta_0$ and $\eta = -\eta_0$, respectively, if the parameters c, $\eta_0 > 0$ are determined from

$$\cosh \eta_0 = 1 + \tfrac{1}{2}\epsilon_{\alpha\beta}, \qquad c = a \sinh \eta_0. \tag{2.12}$$

Any regular harmonic function inside the sphere S_α can be written in the form (Morse & Feshbach 1953)

$$(\cosh \eta - \mu)^{1/2} \sum_{n=0}^\infty A_n \mathrm{e}^{-(n+1/2)\eta} P_n(\mu), \tag{2.13}$$

where $P_n(\mu)$ is the Legendre polynomial of degree n and A_n are unknown coefficients. Since only the local analysis for $\epsilon_{\alpha\beta} \ll 1$ is of interest, the relations (2.11) can be simplified in the near-contact region $z = O(\epsilon_{\alpha\beta} a)$, $r = O(\epsilon_{\alpha\beta}^{1/2} a)$:

$$z = \frac{a\epsilon_{\alpha\beta}^{1/2} \eta}{1-\mu}, \qquad r = \frac{a\epsilon_{\alpha\beta}^{1/2} \sin \xi}{1-\mu}, \tag{2.14}$$

taking into account that $\eta_0 \approx \epsilon_{\alpha\beta}^{1/2}$.

Accordingly, the simplified form of (2.13) can be used to represent the temperature perturbation $T - T_\alpha$ inside S_α in the near-contact region

$$T' - T_\alpha = (1-\mu)^{1/2} \sum_{n=0}^{\infty} A_n \exp\left[-\frac{(n+1/2)(1-\mu)z}{a\epsilon_{\alpha\beta}^{1/2}}\right] P_n(\mu), \tag{2.15}$$

with the prime marking the values related to the disperse phase. The normal component of the flux density on S_α can be derived from (2.15),

$$-\Lambda' \frac{\partial T'}{\partial n}\bigg|_{S_\alpha} \approx \frac{-(1-\mu)^{3/2}}{a\epsilon_{\alpha\beta}^{1/2}} \Lambda' \sum_{n=0}^{\infty} A_n (n+\tfrac{1}{2}) P_n(\mu). \tag{2.16}$$

On the other hand, this flux density can be estimated from an approximately linear behaviour of T^{e} across the gap and the relations (2.2) as

$$\Lambda^{\mathrm{e}}(T_\alpha - T_\beta)(1-f)/(h_{\alpha\beta} + r^2/a). \tag{2.17}$$

Equation (2.15) applied to S_α and the definition (2.2) yield

$$(T_\beta - T_\alpha) f \approx 2(1-\mu)^{1/2} \sum_{n=0}^{\infty} A_n P_n(\mu). \tag{2.18}$$

Using (2.18), the identity

$$1 = \sqrt{2(1-\mu)} \sum_{n=0}^{\infty} P_n(\mu) \tag{2.19}$$

and the near-contact approximation

$$h_{\alpha\beta} + \frac{r^2}{a} \approx \frac{2\epsilon_{\alpha\beta} a}{1-\mu}, \tag{2.20}$$

the flux density (2.17) can be written as

$$\frac{\Lambda^{\mathrm{e}}(1-\mu)^{3/2}}{2\epsilon_{\alpha\beta} a} \sum_{n=0}^{\infty} [\sqrt{2}(T_\alpha - T_\beta) + 2A_n] P_n(\mu). \tag{2.21}$$

Comparing (2.16) and (2.21) yields a simple equation for A_n, resulting in the analytical form for $f(\sigma)$:

$$f(\sigma) = \sqrt{2(1-\mu)} \sum_{n=0}^{\infty} \frac{P_n(\mu)}{1 + (n+\frac{1}{2})\sqrt{\lambda}}, \qquad \sigma = \left[\frac{\lambda(1+\mu)}{1-\mu}\right]^{1/2}. \tag{2.22}$$

The function (2.9),

$$P(\lambda) = \int_{-1}^{1} \frac{f(\sigma)\,\mathrm{d}\mu}{1-\mu} \tag{2.23}$$

can be obtained by termwise integration of (2.22), using (2.19) and the orthogonality properties of the Legendre polynomials,

$$P(\lambda) = 4 \sum_{n=0}^{\infty} \frac{1}{(2n+1)[1 + (n+\frac{1}{2})\sqrt{\lambda}]}. \tag{2.24}$$

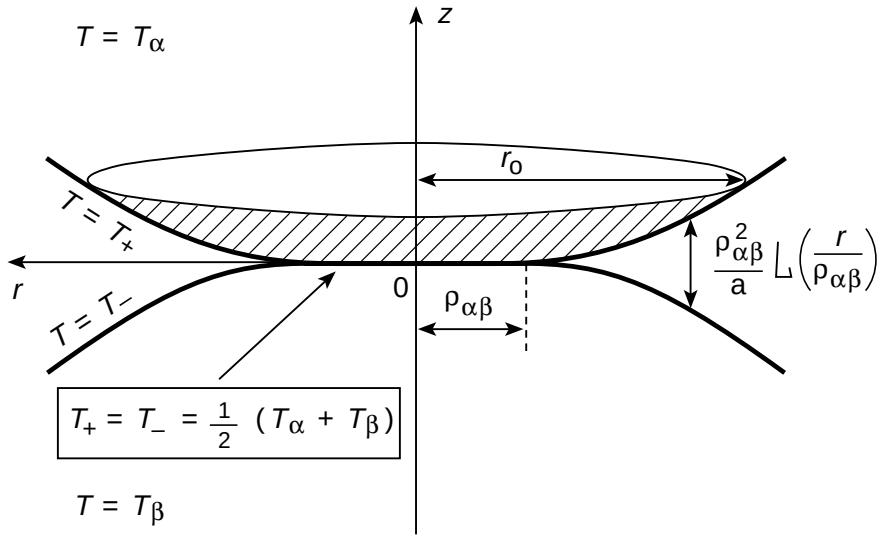

Figure 2. On the calculation of the local thermal flux between two touching, nearly rigid highly conducting spheres.

Expanding each term of (2.24) into primitive fractions, we can express $P(\lambda)$ via the logarithmic derivative $\psi(z)$ of the gamma function (Abramowitz & Stegun 1964),

$$P(\lambda) = 2\left[\psi\left(\frac{1}{2} + \frac{1}{\sqrt{\lambda}}\right) - \psi(\tfrac{1}{2})\right], \tag{2.25}$$

where $\psi(\frac{1}{2}) = -C - 2\ln 2$ and $C = 0.5772\ldots$ is the Euler constant. Using the asymptotic form (Abramowitz & Stegun 1964)

$$\psi(z) \sim \ln z - \frac{1}{2z} - \frac{1}{12z^2} \quad \text{for } z \to \infty, \tag{2.26}$$

we easily arrive at

$$P(\lambda) \sim \ln \lambda^{-1} + 3.9270 + \tfrac{1}{12}\lambda + O(\lambda^2) \quad \text{for } \lambda \to 0, \tag{2.27}$$

which compares well with the approximate result (2.10) of Batchelor & O'Brien.

Finally, (2.6), (2.8), and (2.27) yield the necessary expression for the local flux between two touching highly conducting spheres:

$$\pi \Lambda^{\mathrm{e}} a (T_\alpha - T_\beta)\left[\ln \frac{r_0^2}{a^2} + \ln \gamma^2 - 3.927\right]. \tag{2.28}$$

(*b*) *Two spheres with a small contact spot*

If the spherical particles of surfaces S_α and S_β are pressed together to form a small circular contact spot of radius $\rho_{\alpha\beta} \ll a$ (figure 2), then the integral equation (2.4) is modified to (Batchelor & O'Brien 1977)

$$f(\eta) = -\int_0^1 g(\eta') I\left(\frac{\eta'}{\eta}\right) \mathrm{d}\eta' + \frac{1}{\xi}\int_1^\infty \frac{1 - f(\eta')}{L(\eta')} I\left(\frac{\eta'}{\eta}\right) \mathrm{d}\eta', \tag{2.29}$$

where $\eta = r/\rho_{\alpha\beta}$, $\eta' = r'/\rho_{\alpha\beta}$, $\xi = \gamma\rho_{\alpha\beta}/a$,

$$g(\eta) = \frac{\rho_{\alpha\beta}}{(T_\alpha - T_\beta)} \frac{\partial T'}{\partial n}(r) \tag{2.30}$$

is the non-dimensional normal temperature gradient at the circle of contact and

$$L(\eta) = \frac{2}{\pi}\{(\eta^2-1)^{1/2} + (\eta^2-2)\arctan(\eta^2-1)^{1/2}\} \tag{2.31}$$

is the thickness of the matrix layer scaled with $\rho_{\alpha\beta}^2/a$ (see figure 2) and provided by the elasticity theory. The equation (2.29) is complemented by the temperature continuity condition $T_+ = T_-$ at the circle of contact, which is equivalent to

$$f(\eta) = 1 \quad \text{for } 0 \leqslant \eta \leqslant 1. \tag{2.32}$$

A combination of (2.29) and (2.32) yields a system of equations that can be solved numerically to determine $g(\eta)$ for $0 \leqslant \eta \leqslant 1$ and $f(\eta)$ for $\eta \geqslant 1$.

The flux through an extended circular portion $D_{\alpha\beta}$ of S_α (shadowed in figure 2), with the cut-off radius r_0 in the region of overlapping with the outer solution (§ 3), can be represented as

$$\pi\Lambda^{\mathrm{e}} a(T_\alpha - T_\beta)\left[\ln\frac{r_0^2}{a^2} + \ln\gamma^2 - 3.927 + H_{\mathrm{c}}(\xi) + \Delta H_{\mathrm{m}}(\xi) + o(1)\right], \tag{2.33}$$

where

$$H_{\mathrm{c}}(\xi) = -2\xi\int_0^1 g(\eta)\eta\,\mathrm{d}\eta \tag{2.34}$$

is the contact spot contribution, and

$$\Delta H_{\mathrm{m}}(\xi) = 2\int_1^\infty \left\{\frac{1-f(\eta)}{L(\eta)} - \frac{1-f_0(\xi\eta)}{\eta^2}\right\}\eta\,\mathrm{d}\eta - 2\int_0^1 \frac{1-f_0(\xi\eta)}{\eta}\,\mathrm{d}\eta \tag{2.35}$$

is the difference between the dimensionless flux across the matrix layer and the total flux between particles in point contact. Here $f_0(\sigma)$ is the solution of (2.4) at $\lambda \to 0$. The numerical calculations of Batchelor & O'Brien (1977) for $\xi = 10^{-2}$, 10^{-1}, 1, 10, and 100 demonstrate the qualitative behaviour of $H_{\mathrm{c}}(\xi)$ and $\Delta H_{\mathrm{m}}(\xi)$. However, it is not easy to use these limited data for calculating $H_{\mathrm{c}}(\xi) + \Delta H_{\mathrm{m}}(\xi)$ at arbitrary ξ, which is necessary in our conductivity simulations (§ 6), because, for example, the variation of $H_{\mathrm{c}}(\xi)$ in the important range $1 \leqslant \xi \leqslant 10^2$ is nearly three orders of magnitude. For this reason, we have extended their calculations, using a somewhat different technique, to get complete information about $H_{\mathrm{c}}(\xi) + \Delta H_{\mathrm{m}}(\xi)$.

As noted by Batchelor & O'Brien, the difference $f(\eta) - f_0(\xi\eta)$ between the solutions for deformed and non-deformed particles decays at $\eta \to \infty$ much faster than $f(\eta)$ does. So, using (2.4) at $\lambda = 0$, we replace (2.29) and (2.32) by the system

$$1 - \phi(\eta)L(\eta) = \frac{1}{\xi}\int_1^\infty \left[\phi(\eta') - \frac{1-f_0(\xi\eta')}{\eta'^2}\right] I\left(\frac{\eta'}{\eta}\right)\mathrm{d}\eta' - \int_0^1 g_1(\eta') I\left(\frac{\eta'}{\eta}\right)\mathrm{d}\eta' + f_0(\xi\eta) \qquad (\text{for } 0 < \eta < \infty), \tag{2.36a}$$

$$\phi(\eta) = 0 \qquad (\text{for } \eta \leqslant 1) \tag{2.36b}$$

for the unknowns

$$\phi(\eta) = \frac{1 - f(\eta)}{L(\eta)}, \qquad g_1(\eta) = g(\eta) + \frac{1 - f_0(\xi\eta)}{\xi\eta^2}, \tag{2.37}$$

with improved convergence at $\eta \to \infty$. Instead of a less accurate numerical solution of (2.4) at $\lambda \to 0$, we use for $f_0(\sigma)$ analytical expressions derived from (2.22) at $\lambda \to 0$, σ fixed. In this case, $\mu \approx 1$ and only large n contribute to (2.22). Using the asymptotic relation between $P_n(x)$ and the Bessel function $J_0(x)$ (10.14(6) of Bateman & Erdelyi 1953),

$$P_n(1 - \delta) \approx J_0(n\sqrt{2\delta}) \qquad (\delta \to 0, n \to \infty, n\sqrt{\delta} = O(1)), \tag{2.38}$$

and proceeding in (2.22) from summation to integration, we have

$$f_0(\sigma) = \int_0^\infty \frac{J_0(t)\,\mathrm{d}t}{1 + \frac{1}{2}\sigma t}, \tag{2.39}$$

or, using integration by parts, a better convergent integral

$$f_0(\sigma) = \int_0^\infty \frac{J_1(t)}{t} \frac{(1 + \sigma t)}{(1 + \frac{1}{2}\sigma t)^2}\,\mathrm{d}t. \tag{2.40}$$

The form (2.40), however, is inefficient for small σ. Using

$$J_0(t) = \left(\frac{1}{t}\frac{\mathrm{d}}{\mathrm{d}t}\right)^n [t^n J_n(t)], \tag{2.41}$$

we can generalize (2.40),

$$f_0(\sigma) = (-1)^n \int_0^\infty t^n J_n(t)\,\mathrm{d}t \left(\frac{\mathrm{d}}{\mathrm{d}t}\frac{1}{t}\right)^n \frac{1}{1 + \frac{1}{2}\sigma t} \tag{2.42}$$

and easily calculate all the derivatives $f_0^{(k)}(0)$ from (2.42). In this manner, the asymptotic expansion is found,

$$f_0(\sigma) \sim \sum_{m=0}^{\infty} (-1)^m [(2m-1)!!]^2 (\tfrac{1}{2}\sigma)^{2m}, \qquad \sigma \to 0. \tag{2.43}$$

Finally, the divergent asymptotic series (2.43) is transformed into a convergent, computer-generated continued fraction

$$a_0/(1 + a_1 y/(1 + \cdots \tag{2.44}$$

(where $y = (\sigma/2)^2$), to calculate $f_0(\sigma)$ for $\sigma < 0.35$ (with 35 terms providing at least 5-digit accuracy for $1 - f_0(\sigma)$). For $\sigma > 0.35$, direct integration (2.40) is used.

The logarithmic singularity in the kernel $I(\eta'/\eta)$ is subtracted and accounted for analytically, as usual. The remaining integrals in (2.36 *a*) are approximated to the second order on uniform meshes after the transformations to new variables t and τ:

$$t = 1 - (1 - \eta)^{1/2} \quad \text{for } 0 < \eta < 1, \qquad \tau = [\eta(\eta - 1)]^{1/4} \quad \text{for } \eta > 1, \tag{2.45}$$

with necessary resolutions in the edge region $\eta \approx 1$. Up to 400 nodes in each of the two segments were used, with the cut-off distance $\eta_{\max}$ in (2.36 *a*) up to 400, and the system for unknowns was solved by Gauss elimination (an iterative solution was found to be unsuccessful). Our calculations of $H_c(\xi)$ and $\Delta H_m(\xi)$ are in

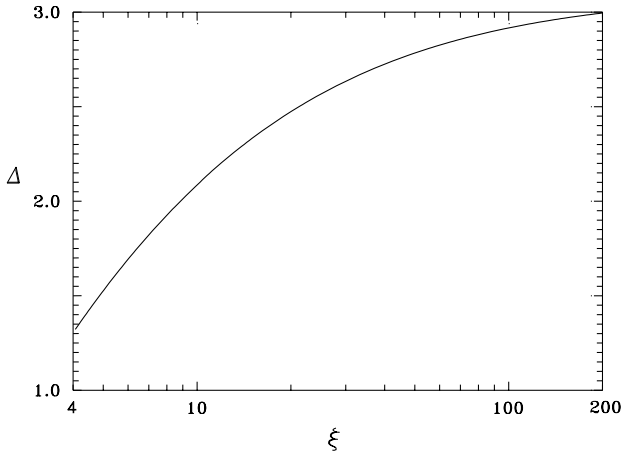

Figure 3. The contact spot function $\Delta(\xi)$.

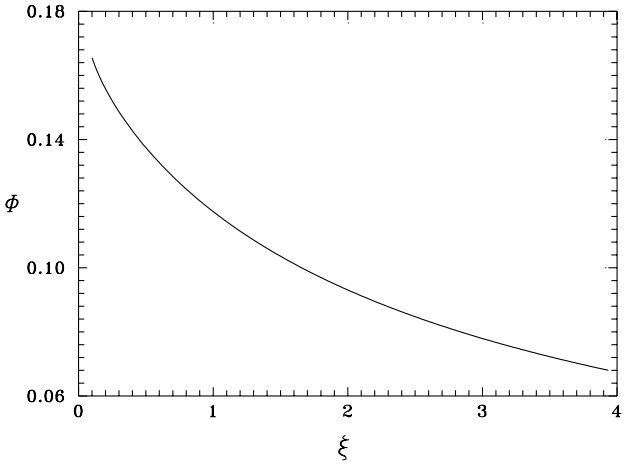

Figure 4. The contact spot function $\Phi(\xi)$.

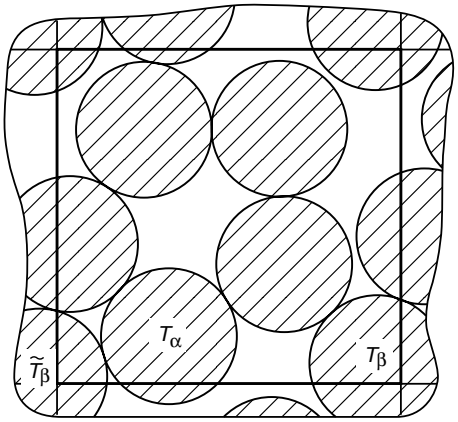

Figure 5. Two-dimensional sketch of a random, triply periodic contact network of spheres.

Table 1. *The values of* $\Delta(\xi)$

(The estimated error in $\Delta(\xi)$ does not exceed 0.1%.)

$\xi = 3.935$	4.067	4.204	4.345	4.491	4.641	4.797	4.958	5.124
1.288	1.322	1.356	1.389	1.422	1.455	1.487	1.518	1.550
$\xi = 5.296$	5.474	5.658	6.044	6.457	6.897	7.368	8.135	9.283
1.580	1.610	1.640	1.698	1.755	1.809	1.862	1.939	2.034
$\xi = 10.594$	12.495	14.738	17.966	21.901	26.699	32.547	39.676	48.367
2.126	2.229	2.323	2.424	2.513	2.592	2.662	2.723	2.776
$\xi = 58.962$	71.877	87.622	106.81	130.21	158.73	193.50	$\xi \to \infty$	
2.822	2.862	2.896	2.93	2.95	2.97	2.99	≈ 3	

Table 2. *The values of* $\Phi(\xi)$

(These values of $\Phi(\xi)$ are accurate to within 3% for $\xi < 0.254$ and 1.3–0.12% for $0.3 < \xi < 4$; the absolute error of $\xi^2\Phi(\xi)$ is within 0.0013 in the whole range of ξ.)

$\xi \to 0$	$\xi = 0.101$	0.150	0.208	0.254	0.300	0.403	0.508	0.599
≈ 0.17	0.16	0.16	0.15	0.15	0.149	0.143	0.137	0.133
$\xi = 0.707$	0.807	0.921	1.017	1.199	1.414	1.614	1.8417	2.0334
0.128	0.124	0.120	0.117	0.111	0.106	0.101	0.0961	0.0924
$\xi = 2.2451$	2.3983	2.6480	2.8287	3.0218	3.2280	3.4483		
0.0888	0.0863	0.0826	0.0801	0.0777	0.0752	0.0728		
$\xi = 3.6837$	3.9351							
0.0704	0.0680							

general agreement with those of Batchelor & O'Brien (1977) for $\xi = 10^{-2}$, 10^{-1}, 1, 10, and 100, although their figure 5 does not allow for an exact comparison. They found considerable convergence difficulties in calculating H_c and ΔH_m; however, our computations show that the sum $H_c + \Delta H_m$, the only quantity of interest, converges much better than H_c and ΔH_m. According to Batchelor & O'Brien, $H_c \sim 2\xi/\pi$ and $\Delta H_m \sim -2\ln\xi$ at $\xi \to \infty$, while H_c, $\Delta H_m = O(\xi^2)$ for $\xi \to 0$. So, it is convenient to define new functions Δ and Φ,

$$H_c(\xi) + \Delta H_m(\xi) = \frac{2\xi}{\pi} - 2\ln\xi + \Delta(\xi) = \xi^2\Phi(\xi), \tag{2.46}$$

the first one being slowly varying for $\xi > 4$ (see table 1 and figure 3), the second one for $\xi < 4$ (table 2 and figure 4). So, unlike $H_c + \Delta H_m$, both functions Δ and Φ can be easily interpolated, thus providing accurate values of the local flux (2.33) for arbitrary ξ.

3. Matched asymptotic expansion strategy for conductivity simulations

It follows from (2.33) that, under most practical conditions ($\gamma\rho_{\alpha\beta}/a \leqslant O(\ln\alpha^2)$), the flux through near-contact areas is only logarithmically large compared to that through the outer region (far from contacts), and so the complicated multiparticle boundary-value problem for the outer region also has to be considered. To succeed, we will use the concepts of matched asymptotic expansions, although our method

will remain heavily numerical. Consider a basic system of particles with surfaces $S_1, \ldots, S_N$ whose centres $\boldsymbol{x}^1, \ldots, \boldsymbol{x}^N$ are in a cubic cell V (of unit side, for simplicity), with triply periodic continuation into all space. As usual in simulations of locally homogeneous systems, periodic boundaries are mandatory to promote convergence $N \to \infty$. The distributions of contact spot radii $\rho_{\alpha\beta}$ are identical in all replicas of the basic periodic cell V (the calculation of $\rho_{\alpha\beta}$ is considered in § 4), while the temperature field has the form

$$T(\boldsymbol{x}) = \boldsymbol{K} \cdot \boldsymbol{x} + T^*(\boldsymbol{x}), \tag{3.1}$$

where $T^*(\boldsymbol{x})$ is triply periodic and the average temperature gradient $\boldsymbol{K}$ is given. When $\gamma \gg 1$ and $\rho_{\alpha\beta}/a \ll 1$, there are two characteristic regions. Far from the contacts (outer region), the particles may be assumed to be spherical, of unperturbed radius a, having *uniform* temperatures ($T_1, \ldots, T_N$ in the basic cell V) and forming a random close packing with *point* contacts (see figure 5 as a two-dimensional illustration). Near the contacts (inner regions), the particle temperatures have significant spatial variations, and finite particle deformations may also have substantial effects.

A further difficulty is that the outer temperatures $T_1, \ldots, T_N$ are unknown and coupled to the behaviour of the solution in the inner regions, via the condition of zero net flux through each particle. To derive the system of equations for $T_1, \ldots, T_N$, consider for each non-deformed sphere $S^0_\alpha (1 \leqslant \alpha \leqslant N)$ a set $\mathcal{A}_\alpha$ of neighbours, i.e. $\beta \in \mathcal{A}_\alpha (1 \leqslant \beta \leqslant N)$, if either S^0_β or its nearest periodic image centred at $\boldsymbol{x}^\beta + \boldsymbol{k}_{\alpha\beta}$ (where $\boldsymbol{k}_{\alpha\beta}$ is a suitable integer displacement vector or zero) is in contact with S^0_α. For any *given* $T_1, \ldots, T_N$, the outer thermal boundary-value problem is well-posed (as can be seen from the solution for two touching superconducting spheres at different temperatures T_1, T_2 in tangent-sphere coordinates), but the flux through any sphere S^0_α, calculated from the outer solution, diverges logarithmically due to the near-contact behaviour

$$\frac{\partial T^{\mathrm{e}}}{\partial n}(\boldsymbol{x})_{|S^0_\alpha} \sim \frac{a(\tilde{T}_\beta - T_\alpha)}{|\boldsymbol{x} - \boldsymbol{x}^c_{\alpha\beta}|^2}, \qquad \boldsymbol{x} \to \boldsymbol{x}^c_{\alpha\beta} \tag{3.2}$$

(see (4.2) of Batchelor & O'Brien (1977) at $h \to 0$), where $\tilde{T}_\beta = T_\beta + \boldsymbol{K} \cdot \boldsymbol{k}_{\alpha\beta}$ is the neighbour temperature and $\boldsymbol{x}^c_{\alpha\beta}$ is the contact point. A proper way to represent the outer solution contribution to the flux through S_α is to cut off small spherical segments $D^0_{\alpha\beta}$ of radius $r_0 \ll a$ (similar to that shown in figure 2) around the contact points with all the neighbours and write the flux through the remaining part of S^0_α as

$$Q_\alpha - \Lambda^{\mathrm{e}} a \sum_{\beta \in \mathcal{A}_\alpha} (\tilde{T}_\beta - T_\alpha) \int_{S^0_\alpha \setminus D^0_{\alpha\beta}} \frac{\mathrm{d}S}{|\boldsymbol{x} - \boldsymbol{x}^c_{\alpha\beta}|^2} + o(1), \tag{3.3}$$

where the first term (the 'flux defect'),

$$Q_\alpha = -\Lambda^{\mathrm{e}} \int_{S^0_\alpha} \left[\frac{\partial T^{\mathrm{e}}}{\partial n}(\boldsymbol{x}) - \sum_{\beta \in \mathcal{A}_\alpha} \frac{a(\tilde{T}_\beta - T_\alpha)}{|\boldsymbol{x} - \boldsymbol{x}^c_{\alpha\beta}|^2} \right] \mathrm{d}S, \tag{3.4}$$

is made a convergent integral over the whole surface S^0_α by subtracting the sum of the contact point contributions from the integrand, and the second term accounts for the logarithmic singularity when $r_0/a \to 0$. The remainder, $o(1)$, tends to zero as $r_0/a \to 0$ and is insignificant.

When (3.3) is added to the inner solution contributions (2.33) (with T_β replaced by $\tilde{T}_\beta$), the logarithmic singularity in r_0/a cancels, as expected, since

$$\lim_{r_0/a\to 0}\left[\frac{1}{\pi}\int_{S_\alpha^0\setminus D_{\alpha\beta}^0}\frac{\mathrm{d}S}{|\boldsymbol{x}-\boldsymbol{x}_{\alpha\beta}^c|^2}+\ln\left(\frac{r_0}{a}\right)^2\right]=2\ln 2 \tag{3.5}$$

and, irrespective of the cut-off radius r_0, the heat balance (zero net flux) for particle α takes the form

$$Q_\alpha-\Lambda^{\mathrm{e}}\pi a\sum_{\beta\in\mathcal{A}_\alpha}(\tilde{T}_\beta-T_\alpha)[2\ln 2+\Psi_{\alpha\beta}]=0, \tag{3.6}$$

where, for brevity,

$$\Psi_{\alpha\beta}=\ln\gamma^2-3.927+H_{\mathrm{c}}\left(\frac{\gamma\rho_{\alpha\beta}}{a}\right)+\Delta H_{\mathrm{m}}\left(\frac{\gamma\rho_{\alpha\beta}}{a}\right). \tag{3.7}$$

Matched asymptotic expansions can be also used to represent the average thermal flux $\langle\boldsymbol{q}\rangle$ through a granular material, starting from the exact relation of Batchelor & O'Brien

$$\langle\boldsymbol{q}\rangle=-\Lambda^{\mathrm{e}}\left[\boldsymbol{K}+\frac{(1-\gamma^{-1})}{V}\sum_{\alpha=1}^{N}\int_{S_\alpha}(\boldsymbol{x}-\boldsymbol{x}^\alpha)\frac{\partial T^{\mathrm{e}}}{\partial n}\,\mathrm{d}S\right] \tag{3.8}$$

(V is the cell volume, unity in our case), where $\boldsymbol{x}^\alpha$ is arbitrary and can be taken as the centre of the non-deformed sphere S_α^0. In the inner regions, $\boldsymbol{x}-\boldsymbol{x}^\alpha$ can be replaced by $a\boldsymbol{n}_{\alpha\beta}$ (where $\boldsymbol{n}_{\alpha\beta}$ is the unit centre-to-centre director from S_α^0 to its neighbour) with a small relative error in the integral (3.8), on the order $O(r_0^2/a^2)$. Thus, the inner solution contribution to the integral (3.8) can be found as the weighted sum of expressions (2.33) (with $\tilde{T}_\beta$ instead of T_β).

The outer solution contribution is similar to (3.3)–(3.4), with an additional factor $a\boldsymbol{n}$ in the integrands. Summing these contributions and using the relation

$$\lim_{r_0/a\to 0}\left[\frac{1}{\pi}\int_{S_\alpha^0\setminus D_{\alpha\beta}^0}\frac{\boldsymbol{n}\,\mathrm{d}S}{|\boldsymbol{x}-\boldsymbol{x}_{\alpha\beta}^c|^2}+\boldsymbol{n}_{\alpha\beta}\ln\left(\frac{r_0}{a}\right)^2\right]=2(\ln 2-1)\boldsymbol{n}_{\alpha\beta}, \tag{3.9}$$

we can approximate the integral (3.8) as

$$\int_{S_\alpha}(\boldsymbol{x}-\boldsymbol{x}^\alpha)\frac{\partial T^{\mathrm{e}}}{\partial n}\,\mathrm{d}S\approx W_\alpha+\pi a^2\sum_{\beta\in\mathcal{A}_\alpha}(\tilde{T}_\beta-T_\alpha)[2\ln 2-2+\Psi_{\alpha\beta}]\boldsymbol{n}_{\alpha\beta}, \tag{3.10}$$

where

$$W_\alpha=a\int_{S_\alpha^0}\left[\frac{\partial T^{\mathrm{e}}}{\partial n}(\boldsymbol{x})-\sum_{\beta\in\mathcal{A}_\alpha}\frac{a(\tilde{T}_\beta-T_\alpha)}{|\boldsymbol{x}-\boldsymbol{x}_{\alpha\beta}^c|^2}\right]\boldsymbol{n}\,\mathrm{d}S, \tag{3.11}$$

the 'thermal dipole defect', is another convergent integral determined by the outer solution.

In principle, the relations (3.4) and (3.6) for $\alpha=1,\ldots,N$, together with (3.1) and the Laplace equation $\nabla^2T=0$ outside the spheres, make the outer problem uniquely soluble, to within an insignificant additive constant in $T^{\mathrm{e}}(\boldsymbol{x})$ and $T_1,\ldots,T_N$. However, even numerically, it is extremely difficult to find a satisfactory solution for this singular problem, because the multipole method in this case is divergent. The

central idea of our approach is to slightly contract the radius of all spheres in the outer geometry from a to $\hat{a} = 2a/(\epsilon+2)$, where $\epsilon \ll 1$, thus making a small *artificial* gap $\epsilon\hat{a}$ between formerly contacting neighbours, and consider thermal conduction through this system of non-touching superconducting spheres $\hat{S}_\alpha$ in the matrix, with the same (yet unknown) boundary temperatures $T_1, \ldots, T_N$, as in (3.4) and (3.6) for touching spheres. On doing this, we can use, with a very small error as $\epsilon \to 0$, the difference between the net (convergent!) flux through the sphere $\hat{S}_\alpha$ and the sum of the gap contributions from all its former neighbours to calculate the flux defect for touching spheres, the most difficult first term in (3.6). (As a further motivation of this idea, a curious analogy with two-sphere Stokesian hydrodynamics in close approach (Cooley & O'Neill 1969) can be mentioned: the $O(1)$-terms in the singular resistance coefficients, as $\epsilon \to 0$, can be calculated by using the outer solution for two *touching* spheres but, alternatively, and with an error of $O(\epsilon \ln \epsilon)$, as the difference between the exact solution for non-touching spheres and the sum of the singular terms.)

To realize this approach, we can again apply matched asymptotic expansions to this new system of non-touching superconducting spheres and represent the flux through $\hat{S}_\alpha$ as the sum of the inner and outer solution contributions. A typical inner solution contribution is obtained from (2.8), with $P = 0$ and a replaced by $\hat{a}$:

$$\pi \Lambda^{\mathrm{e}} \hat{a} (T_\alpha - \tilde{T}_\beta) \left[\ln \frac{r_0^2}{a^2} + \ln \epsilon^{-1} + o(1) \right]. \tag{3.12}$$

The outer solution contribution, to the leading order of approximation, is the same as for touching superconducting spheres (3.3)–(3.4). Thus, for $\epsilon \ll 1$,

$$-\Lambda^{\mathrm{e}} \int_{\hat{S}_\alpha} \frac{\partial T^{\mathrm{e}}}{\partial n} \, \mathrm{d}S = Q_\alpha - \Lambda^{\mathrm{e}} \pi a \sum_{\beta \in \mathcal{A}_\alpha} (\tilde{T}_\beta - T_\alpha) \left[2 \ln 2 + \frac{\hat{a}}{a} \ln \epsilon^{-1} \right] + o(1). \tag{3.13}$$

The flux defect Q_α can be excluded from (3.6) and (3.13), resulting in

$$\int_{\hat{S}_\alpha} \frac{\partial T^{\mathrm{e}}}{\partial n} \, \mathrm{d}S + \sum_{\beta \in \mathcal{A}_\alpha} H_{\alpha\beta} (\tilde{T}_\beta - T_\alpha) \approx 0, \tag{3.14}$$

with

$$H_{\alpha\beta} = \pi a \left(\Psi_{\alpha\beta} - \frac{\hat{a}}{a} \ln \epsilon^{-1} \right). \tag{3.15}$$

Similarly, the thermal dipole in the system of non-touching superconducting spheres can be approximated for $\epsilon \ll 1$ as

$$\int_{\hat{S}_\alpha} (\boldsymbol{x} - \boldsymbol{x}^\alpha) \frac{\partial T^{\mathrm{e}}}{\partial n} \, \mathrm{d}S = W_\alpha + \pi a^2 \sum_{\beta \in \mathcal{A}_\alpha} (\tilde{T}_\beta - T_\alpha) \left[2 \ln 2 - 2 + \left(\frac{\hat{a}}{a} \right)^2 \ln \epsilon^{-1} \right] \boldsymbol{n}_{\alpha\beta} + o(1), \tag{3.16}$$

and, upon exclusion of W_α from (3.10) and (3.16), we have

$$\int_{S_\alpha} (\boldsymbol{x} - \boldsymbol{x}^\alpha) \frac{\partial T^{\mathrm{e}}}{\partial n} \, \mathrm{d}S \approx \int_{\hat{S}_\alpha} (\boldsymbol{x} - \boldsymbol{x}^\alpha) \frac{\partial T^{\mathrm{e}}}{\partial n} \, \mathrm{d}S + \pi a^2 \sum_{\beta \in \mathcal{A}_\alpha} (\tilde{T}_\beta - T_\alpha) \left[\Psi_{\alpha\beta} - \left(\frac{\hat{a}}{a} \right)^2 \ln \epsilon^{-1} \right] \boldsymbol{n}_{\alpha\beta}. \tag{3.17}$$

The error of the relations (3.14) and (3.17) is expected to be $O(\epsilon \ln \epsilon)$, since the asymptotic analysis (Appendix A) of the standard potential problem for two isolated, nearly touching superconducting spheres $\hat{S}_\alpha$ and $\hat{S}_\beta$ with temperature difference ΔT shows that both the surface integrals

$$\int \frac{\partial T^{\mathrm{e}}}{\partial n}\,\mathrm{d}S, \qquad \int \boldsymbol{n}\frac{\partial T^{\mathrm{e}}}{\partial n}\,\mathrm{d}S \tag{3.18}$$

over $\hat{S}_\alpha$ or $\hat{S}_\beta$ have the structure $\hat{a}\Delta T[c_0 \ln \epsilon + c_1 + O(\epsilon \ln \epsilon)]$ at $\epsilon \to 0$, with some constants c_0, c_1. The use of $\hat{a}/a$ instead of unity in (3.15) and (3.17) is not of principal importance, but is believed to reduce the error of (3.14) and (3.17) (see Appendix A).

We can consider (3.14) as exact relations, making the boundary-value problem for non-touching superconductors uniquely soluble (see below), to within an insignificant additive constant, and use the solution to calculate $\langle \boldsymbol{q} \rangle$ for the original problem from (3.8) and (3.17) with an error $O(\epsilon \ln \epsilon)$, and then take the limit $\epsilon \to 0$. Thus, (3.14) and (3.17) can be called the consistency conditions, since they relate the asymptotic solution of the original problem for touching, highly conducting particles with possible small contact deformations to the solution of the different problem for non-touching, non-deformed superconducting spheres; finite particle conductivity and elasticity are effectively accounted for in the 'heat–transfer' coefficients $H_{\alpha\beta}$. Using Green's theorem, one can easily prove that (3.14) is a well-posed problem for $H_{\alpha\beta} > 0$, i.e. only for $\epsilon > 50.8/\gamma^2$ in the case $\rho_{\alpha\beta} = 0$. However, $H_{\alpha\beta} > 0$ is a sufficient, but not necessary condition, and both our calculations (§ 6) and an analytical solution of the model two-sphere problem (Appendix A) show that (3.14) is a well-posed problem for all $\epsilon > 0$, and so the necessary limit $\epsilon \to 0$ is rigorously defined for every γ.

This is a very efficient procedure, since the progression exponent for the decay of multipole coefficients in a system of nearly touching superconductors is $1 - \sqrt{\epsilon}$ (Zinchenko 1994*a*), not $1 - O(\epsilon)$, and so multipole expansions remain reasonably fast converging even for small ϵ.

We note finally that the proposed approach to conductivity simulations in a granular material is, in fact, semi-asymptotic, i.e. we neglect the corrections like $O(\gamma^{-1})$ due to the temperature non-uniformity inside the inclusions in the outer solution, but take $\ln \gamma$ as a finite parameter. As an alternative, an asymptotic expansion in inverse powers of $\ln \gamma$ could be attempted, but this approach proves to be more difficult and much less efficient (see § 6).

4. Random close packings and the calculation of contact deformations

The conductivity simulations by matched asymptotic expansions, as described in the previous section, require computer–generated random close packings (RCP) of non-deformed spheres $S_1^0, \ldots, S_N^0$ with triply periodic continuation into all space. To this end, we used the algorithm of Zinchenko (1994*b*) and extended his calculations, to prepare more RCP configurations with $N \leqslant 200$ and perfect contactness and also determine contact deformations by the perturbation analysis. The essence of the algorithm is as follows. Let the system initially form a network with $3N - 3$ independent contacts (and each sphere having at least three neighbours). Then the geometric relations $R_{\alpha\beta}^2 = (2a)^2$ (where $\boldsymbol{R}_{\alpha\beta} = \boldsymbol{x}^\beta + \boldsymbol{k}_{\alpha\beta} - \boldsymbol{x}^\alpha$ is the 'minimal vector' drawn from $\boldsymbol{x}^\alpha$ to the centre of the periodically replicated S_β^0 that is nearest to S_α^0)

for all independent contact pairs (α_k, β_k) $(k = 1, \ldots, 3N-3)$ form $3N-3$ nonlinear equations for $3N$ unknowns x^α, y^α, z^α and, in principle, determine sphere positions as unique functions of their radius a, to within an insignificant shift of the whole system and particle permutation. The differentiation of the above geometric relations with respect to a yields a system of *differential equations of densification*,

$$\frac{\mathrm{d}\boldsymbol{x}^\alpha}{\mathrm{d}a} = \boldsymbol{V}_\alpha(\boldsymbol{x}^1, \ldots, \boldsymbol{x}^N, a), \tag{4.1}$$

with $\boldsymbol{V}_\alpha$ determined from

$$\boldsymbol{R}_{\alpha_k,\beta_k} \cdot (\boldsymbol{V}_{\beta_k} - \boldsymbol{V}_{\alpha_k}) = 4a \quad \text{for } k = 1, \ldots, 3N-3, \tag{4.2a}$$

$$\sum_{\alpha=1}^{N} \boldsymbol{V}_\alpha = 0, \tag{4.2b}$$

which can be solved numerically, thus allowing particles to swell while keeping all the existing contacts until a new contact $k = 3N-2$ occurs. At that moment, the addition of the new contact equation makes the system (4.2) for $\boldsymbol{V}_\alpha$ overdetermined, and one of the existing bonds with $k = k^* \leqslant 3N-3$ has to be broken to continue the densification. To this end, we first calculate the extremal point $(\boldsymbol{V}_1^*, \ldots, \boldsymbol{V}_N^*)$ that minimizes the function

$$F(\boldsymbol{V}_1, \ldots, \boldsymbol{V}_N) = \sum_{k=1}^{3N-2} [\boldsymbol{R}_{\alpha_k,\beta_k} \cdot (\boldsymbol{V}_{\beta_k} - \boldsymbol{V}_{\alpha_k}) - 4a]^2 \tag{4.3}$$

by the solution of the linear system

$$\sum_{\beta \in \mathcal{A}_\alpha} [4a - \boldsymbol{R}_{\alpha\beta} \cdot (\boldsymbol{V}_\beta^* - \boldsymbol{V}_\alpha^*)] \boldsymbol{R}_{\alpha\beta} = 0, \qquad \alpha = 1, 2, \ldots, N \tag{4.4}$$

(where $\mathcal{A}_\alpha$ is the set of neighbours of S_α^0, as in § 3) and find the bond $k = k^*$ with maximum $\boldsymbol{R}_{\alpha_k,\beta_k} \cdot (\boldsymbol{V}_{\beta_k}^* - \boldsymbol{V}_{\alpha_k}^*)$ to be excluded from (4.2), with the new bond $k = 3N-2$ added. It was rigorously proved (Zinchenko 1994*b*) that the separation condition

$$\boldsymbol{R}_{\alpha_{k^*},\beta_{k^*}} \cdot (\boldsymbol{V}_{\beta_{k^*}} - \boldsymbol{V}_{\alpha_{k^*}}) > 4a$$

is equivalent to

$$\boldsymbol{R}_{\alpha_{k^*},\beta_{k^*}} \cdot (\boldsymbol{V}_{\beta_{k^*}}^* - \boldsymbol{V}_{\alpha_{k^*}}^*) > 4a,$$

and so, if the latter holds, the densification can be continued until a new contact occurs, and so on. The algorithm terminates when, after a new contact formation, $\boldsymbol{R}_{\alpha_k,\beta_k} \cdot (\boldsymbol{V}_{\beta_k}^* - \boldsymbol{V}_{\alpha_k}^*) - 4a \leqslant 0$ for all $k \leqslant 3N-2$, and so no bond can be separated. A modification of this scheme is used to prepare an initial network with $3N-3$ independent contacts from a random dilute system of non-touching spheres. Technical aspects of the algorithm, some of them complicated, are discussed in detail by Zinchenko (1994*b*). This algorithm is essentially 'static', i.e. it contains no densification rate $\mathrm{d}a/\mathrm{d}t$, and non-crystallizing, due to the conservation of the contact network in the course of densification. Both the random close-packing density and the radial distribution function obtained by this algorithm were found to be in excellent agreement with experimental data. The other geometric or thermodynamic packing codes with periodic boundaries, as discussed by Zinchenko (1994*b*), are *kinetics determined* and can provide any degree of crystallization for sufficiently slow densification.

The Euler scheme used to integrate (4.1) never produces overlaps of bonded particles, but, conversely, makes them slightly non-touching during the bond lifetimes. This latter, undesirable effect, however, can be made arbitrarily small by choosing fine integration steps Δa. In the present work, we used at least an order-of-magnitude smaller integration steps than in Zinchenko (1994*b*) and prepared new RCP configurations with almost perfect contacts for conductivity simulations (among two possible strategies of generating initial approximations $\boldsymbol{V}_\alpha^0$ to $\boldsymbol{V}_\alpha$ at the first densification stage, discussed in § 2.4 of Zinchenko (1994*b*), the strategy with random numbers was chosen to reduce difficulties at the 'singular point', more noticeable for small Δa). Fifteen configurations were generated for $N = 100$ with packing density in the range $0.619 \leqslant c \leqslant 0.639$ and 10 configurations for $N = 200$ with $0.623 \leqslant c \leqslant 0.639$; for all the packings, the average gap between the spheres that should be in contact is only about $5 \times 10^{-7} a$ (several small packings with even better contacts were also prepared for test purposes of § 6). It should be noted that very small integration steps make the computations more expensive (on the average, it took about 25h to prepare one random close packing with $N = 200$ on an IBM AIX RISC/6000 workstation) and also increase the dispersion of the final packings, so that more configurations are required for averaging. However, the average packing densities $\langle c \rangle = 0.628 \pm 0.002 (N = 100)$ and $0.631 \pm 0.002 (N = 200)$ (compared to 0.629 and 0.633 for $N = 100$ and 200, respectively, in Zinchenko (1994*b*)) are again consistent with the experimentally determined limit 0.637 at $N \to \infty$ by Scott & Kilgour (1969). Once generated, these packings can be used in conductivity simulations for all γ and the elastic parameters Π (see (4.9) below).

Most importantly, this isotropic, purely geometric algorithm terminates when the spheres reach mechanical equilibrium under the action of normal contact forces. Indeed, at random close packing, (4.4) can be written as equilibrium equations

$$\sum_{\beta \in \mathcal{A}_\alpha} N_{\alpha\beta} \boldsymbol{R}_{\alpha\beta} = 0, \quad \text{for } \alpha = 1, \ldots, N, \tag{4.5}$$

where

$$N_{\alpha\beta} = -\lambda [\boldsymbol{R}_{\alpha\beta} \cdot (\boldsymbol{V}_\beta^* - \boldsymbol{V}_\alpha^*) - 4a] \tag{4.6}$$

are non-negative normal reactions and $\lambda > 0$ is an arbitrary parameter. In principle, the system of $3N - 3$ independent equations (4.5) determines $3N - 2$ unknown reactions $N_{\alpha\beta}$ to within an arbitrary factor, but (4.6) is a convenient way to bypass (4.5) and reduce the calculation of $N_{\alpha\beta}$ to the solution of the self-adjoint, positive-definite system (4.4) by conjugate gradient iterations. The system of reactions is determined uniquely, if the average pressure $\langle p \rangle$ in the material is specified. Indeed, the pressure $\langle p \rangle$, defined as $-(\mathcal{P}_{11} + \mathcal{P}_{22} + \mathcal{P}_{33})/3$ (where $\mathcal{P}_{ij}$ is the average stress tensor) can be expressed via contact forces in a standard way

$$\langle p \rangle = \frac{2a}{3} \sum_{k=1}^{3N-2} N_{\alpha_k, \beta_k} \tag{4.7}$$

(for unit periodic cell volume), thus determining λ.

These normal reactions between absolutely rigid spheres can be used to calculate small contact deformations from Hertz theory (Landau & Lifshitz 1959), as a

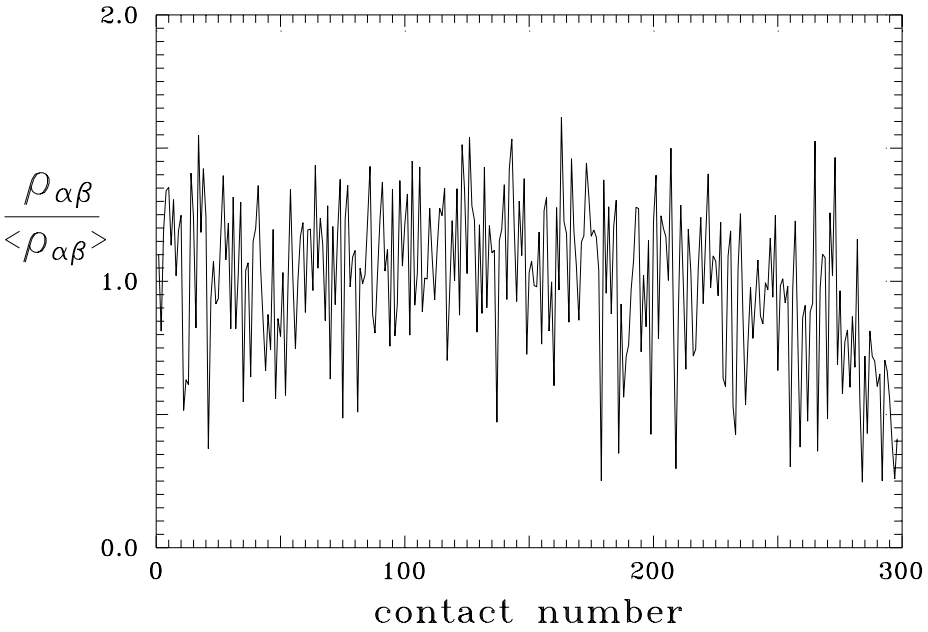

Figure 6. The distribution of contact spot radii $\rho_{\alpha\beta}$ in a random close packing of 100 spheres with $c = 0.627$ in a periodic box, scaled with the average value $\langle\rho_{\alpha\beta}\rangle$ for a given configuration.

geometric perturbation. Contact spot radii are given by

$$\rho_{\alpha\beta} = \left\{\frac{3(1-\nu^2)a}{4E}N_{\alpha\beta}\right\}^{1/3}, \tag{4.8}$$

where E and ν are the material Young's modulus and the Poisson ratio, respectively. According to (4.7)–(4.8), the dimensionless contact spot radii $\rho_{\alpha\beta}/a$ for a given configuration are uniquely determined by the elastic parameter

$$\Pi = \left\{\frac{\langle p\rangle(1-\nu^2)}{E}\right\}^{1/3}. \tag{4.9}$$

Figure 6 and other calculations for random close packings with $N = 100$ and 200 demonstrate that the contact radius distribution is not close to uniform (despite the 1/3 exponent in (4.8)), the standard deviation of $\rho_{\alpha\beta}$ being about 30% of its mean value $\langle\rho_{\alpha\beta}\rangle$. The mean contact radius was found to be

$$\langle\rho_{\alpha\beta}\rangle = 1.25a\Pi, \tag{4.10}$$

where 1.25 is the average over 10 random close packings with $N = 200$ (averaging over 15 RCP configurations with $N = 100$ yields a close value 1.24).

It is very advantageous that the conductivity simulation strategy of § 3 requires only random close packings of absolutely rigid spheres and that the small elasticity is effectively accounted for in the 'heat transfer coefficients' $H_{\alpha\beta}$. If necessary for other purposes, a small correction (on the order $\Pi^2 a$) to the outer geometry, compatible with near-contact deformations, could be calculated by a perturbation analysis, as follows. The application of an isotropic mechanical load to a random close packing with periodic boundaries can be modelled as resulting from some swelling of particle

radius (rather than from the periodic cell compression). Let, in the outer geometry, the sphere centres be $\boldsymbol{x}^\alpha + \delta\boldsymbol{x}^\alpha$ and their radius $a + \delta a$. The centre-to-centre distance between neighbouring spheres becomes approximately $2(a+\delta a) - 2\rho^2_{\alpha\beta}/a$, where the last term accounts for the contact compliance (see, for example, Batchelor & O'Brien 1977). Thus, we arrive at the linearized equations,

$$\boldsymbol{R}_{\alpha_k,\beta_k} \cdot (\delta\boldsymbol{x}^{\beta_k} - \delta\boldsymbol{x}^{\alpha_k}) - 4a\delta a + 4\rho^2_{\alpha_k,\beta_k} = 0 \quad \text{for } k = 1, 2, \ldots, 3N-2. \tag{4.11}$$

These $3N-2$ contact equations uniquely determine $3N+1$ perturbations $\delta\boldsymbol{x}^1, \ldots, \delta\boldsymbol{x}^N$ and δa, to within an insignificant vector constant added to all $\delta\boldsymbol{x}^\alpha$. An efficient numerical technique to solve (4.11) is the conjugate gradient method, as for (4.2) (see Zinchenko 1994*b*).

Since the neighbouring spheres in our computer-generated packings are (very slightly) non-touching, we prefer to modify (3.15) and (3.17) and use $\epsilon_{\alpha\beta}$ instead of $\epsilon = 2(a-\hat{a})/\hat{a}$, where $\epsilon_{\alpha\beta}\,\hat{a}$ is the actual gap between the spheres after the radius contraction. A more serious problem is the existence of 'near-neighbours', besides true (contacting) neighbours, in typical random close packings. For example, if all pairs with $R_{\alpha\beta} < 2.02a$ are qualified as neighbours, then the coordination number (the average number of neighbours per particle) is typically about 6.6 (for $N \gg 1$), compared to $6 - 4/N$ when only true neighbours are accounted for. These near-neighbours can make the necessary values of ϵ too small to accurately achieve the limit $\epsilon \to 0$ in the conductivity simulations, with unacceptably slow convergence of the multipole expansions (§ 5,6). Fortunately, it has proved possible to overcome this difficulty as follows. Fixing some small $\epsilon^0_{\max} > 0$, we define for each sphere S^0_α a set $\mathcal{B}_\alpha$ of near-neighbours with $R_{\alpha\beta} < (2 + \epsilon^0_{\max})a$, not including true neighbours. For each near-neighbour, we subtract its main, logarithmic contribution from the flux through sphere $\hat{S}_\alpha$ in the system of slightly contracted superconductors, but also add a compensating term for the original geometry of random close-packed spheres. A similar manipulation is made with the thermal dipoles. Thus, (3.14) and (3.17) are replaced with

$$\int_{\hat{S}_\alpha} \frac{\partial T^{\mathrm{e}}}{\partial n}\,\mathrm{d}S + \pi a \sum_{\beta\in\mathcal{A}_\alpha} \left(\Psi_{\alpha\beta} - \frac{\hat{a}}{a}\ln\epsilon^{-1}_{\alpha\beta}\right)(\tilde{T}_\beta - T_\alpha) + \pi a \sum_{\beta\in\mathcal{B}_\alpha} \left[\ln(\epsilon^0_{\alpha_\beta})^{-1} - \frac{\hat{a}}{a}\ln\epsilon^{-1}_{\alpha\beta}\right](\tilde{T}_\beta - T_\alpha) = 0 \tag{4.12}$$

and

$$\begin{aligned}\int_{S_\alpha} (\boldsymbol{x}-\boldsymbol{x}^\alpha)\frac{\partial T^{\mathrm{e}}}{\partial n}\,\mathrm{d}S \approx \int_{\hat{S}_\alpha} (\boldsymbol{x}-\boldsymbol{x}^\alpha)\frac{\partial T^{\mathrm{e}}}{\partial n}\,\mathrm{d}S \\ + \pi a^2 \sum_{\beta\in\mathcal{A}_\alpha} (\tilde{T}_\beta - T_\alpha)\left[\Psi_{\alpha\beta} - \left(\frac{\hat{a}}{a}\right)^2 \ln\epsilon^{-1}_{\alpha\beta}\right]\boldsymbol{n}_{\alpha\beta} \\ + \pi a^2 \sum_{\beta\in\mathcal{B}_\alpha} (\tilde{T}_\beta - T_\alpha)\left[\ln(\epsilon^0_{\alpha\beta})^{-1} - \left(\frac{\hat{a}}{a}\right)^2 \ln\epsilon^{-1}_{\alpha\beta}\right]\boldsymbol{n}_{\alpha\beta},\end{aligned} \tag{4.13}$$

where $\epsilon^0_{\alpha\beta}a$ is the gap between the spheres prior to the radius contraction.

While the first modification, $\epsilon_{\alpha\beta}$ instead of ϵ, seems almost insignificant (since $\epsilon_{\alpha\beta} \approx \epsilon$ for $\beta \in \mathcal{A}_\alpha$ and the values of $\epsilon \gg 5 \times 10^{-7}$ used), the inclusion of near-neighbours, as suggested in (4.12)–(4.13), has a drastic effect on the rate of convergence $\epsilon \to 0$ in conductivity simulations (see § 6). The value $\epsilon^0_{\max} = 0.01$ was found to be close to optimal for typical random close packings. It is important to stress that the limiting result for $\epsilon \to 0$ is independent of $\epsilon^0_{\max}$, since the near-neighbour contributions to (4.12)–(4.13) vanish, when $\hat{a} = a$ and $\epsilon_{\alpha\beta} = \epsilon^0_{\alpha\beta}$.

5. Solution of the boundary-value problem

The most difficult part of the conductivity simulations is the solution of the thermal boundary-value problem (4.12) for slightly contracted superconducting spheres and taking the limit $\epsilon \to 0$. A special, high resolution, economical multipole technique has been recently developed by Zinchenko (1994*a*) to solve the problem of thermal conduction through a large random system of N identical spheres with triply periodic continuation into all space, arbitrary particle-to-medium conductivity ratio γ and arbitrary volume fractions. The limiting case $\gamma = \infty$ of that solution obviously corresponds to superconductors with zero net flux through each sphere. The present boundary-value problem is new in that the flux through an individual sphere is non-zero and satisfies (4.12), so additional zero-order harmonics should be included (see (5.5)), but otherwise the solution can be constructed in a similar manner, as briefly summarized below. Further details of this highly efficient, but somewhat lengthy technique can be found in Zinchenko (1994*a*).

Let $G(\boldsymbol{x})$ be the triply periodic Green function satisfying

$$\nabla^2 G(\boldsymbol{x}) = -4\pi + 4\pi \sum_{\boldsymbol{k}} \delta(\boldsymbol{x} - \boldsymbol{k}), \qquad \boldsymbol{k} = (k_1, k_2, k_3), \tag{5.1}$$

where $\delta(\boldsymbol{x})$ is the δ-function and the symbol $\sum$ denotes the summation over all integers k_1, k_2, k_3 (the Cartesian axes are chosen so that the basic periodic cell V is the unit cube $[0,1) \times [0,1) \times [0,1)$). Using Green's theorem, a harmonic, triply periodic function $T_*(\boldsymbol{x}) = T(\boldsymbol{x}) - \boldsymbol{K} \cdot \boldsymbol{x}$ can be represented outside the inclusions as

$$T^{\mathrm{e}}_*(\boldsymbol{x}) = \text{const.} + \frac{1}{4\pi} \sum_{\beta=1}^{N} \int_{\hat{S}_\beta} \left[G(\boldsymbol{y} - \boldsymbol{x}) \frac{\partial T^{\mathrm{e}}_*}{\partial n_{\boldsymbol{y}}} - T_*(\boldsymbol{y}) \frac{\partial G(\boldsymbol{y} - \boldsymbol{x})}{\partial n_{\boldsymbol{y}}} \right] \mathrm{d}S_{\boldsymbol{y}}. \tag{5.2}$$

The temperature uniformity on $\hat{S}_\beta$, Green's theorem for the fields $\boldsymbol{K} \cdot \boldsymbol{y}$ and $G(\boldsymbol{y} - \boldsymbol{x})$ inside $\hat{S}_\beta$, and (5.2) yield

$$T^{\mathrm{e}}(\boldsymbol{x}) = \boldsymbol{K} \cdot \boldsymbol{x} + C + \frac{1}{4\pi} \sum_{\beta=1}^{N} \int_{\hat{S}_\beta} G(\boldsymbol{y} - \boldsymbol{x}) \frac{\partial T^{\mathrm{e}}}{\partial n_{\boldsymbol{y}}}(\boldsymbol{y}) \, \mathrm{d}S_{\boldsymbol{y}}, \tag{5.3}$$

where C is another insignificant constant. The next step is to associate with each sphere $\hat{S}_\alpha$ the local spherical coordinate system (r, θ, ϕ) so that

$$\left.\begin{aligned} (\boldsymbol{x} - \boldsymbol{x}^\alpha)_1 &= r \sin\theta \cos\phi, \\ (\boldsymbol{x} - \boldsymbol{x}^\alpha)_2 &= r \sin\theta \sin\phi, \\ (\boldsymbol{x} - \boldsymbol{x}^\alpha)_3 &= r \cos\theta, \end{aligned}\right\} \tag{5.4}$$

(here and henceforth the number indices of vectors denote their Cartesian components) and a set of complex Fourier coefficients $U^{\alpha}_{n,m}$:

$$\frac{\partial T^{\mathrm{e}}}{\partial n}(\boldsymbol{x})_{|\hat{S}_\alpha} = \sum_{n=0}^{\infty}\sum_{m=-n}^{n} [\pi(2n+1)]^{1/2} U^{\alpha}_{n,m} Y_{nm}(\boldsymbol{x}-\boldsymbol{x}^{\alpha}), \tag{5.5}$$

with

$$U^{\alpha}_{n,-m} = (-1)^m \overline{U}^{\alpha}_{n,m} \tag{5.6}$$

and the overbar denoting complex conjugation. For a vector $\boldsymbol{r} = (r,\theta,\phi)$, the normalized spherical harmonics are defined as

$$\left.\begin{aligned} Y_{nm}(\boldsymbol{r}) &= \left[\frac{(2n+1)(n-m)!}{4\pi(n+m)!}\right]^{1/2} P_n^m(\cos\theta)\exp(\mathrm{i}m\phi) \qquad (m \geqslant 0),\\ Y_{nm}(\boldsymbol{r}) &= (-1)^m \overline{Y}_{n,-m}(\boldsymbol{r}) \qquad\qquad\qquad\qquad\quad (m \leqslant 0), \end{aligned}\right\} \tag{5.7}$$

with P_n^m being the associated Legendre function. To derive a set of equations for $U^{\alpha}_{n,m}$ from (5.3) and (5.5), the integrals

$$I = \int_{\hat{S}_\alpha} \overline{Y}_{nm}(\boldsymbol{x}-\boldsymbol{x}^{\alpha})\,\mathrm{d}\Omega_{\boldsymbol{x}} \frac{\partial}{\partial n_{\boldsymbol{x}}} \int_{\hat{S}_\beta} G(\boldsymbol{y}-\boldsymbol{x}) Y_{\nu\mu}(\boldsymbol{y}-\boldsymbol{x}^{\beta})\,\mathrm{d}\Omega_{\boldsymbol{y}} \qquad (\mathrm{d}\Omega = \mathrm{d}S/\hat{a}^2) \tag{5.8}$$

for all $\nu \geqslant 0$ (the index ν not to be confused with the Poisson ratio) and $n \geqslant 1$ should be evaluated. (Note that the equation for $U^{\alpha}_{0,0}$ is a consequence of the total zero flux through all N spheres.) These integrals can be calculated in different ways, e.g. like similar integrals in Zinchenko (1994*a*). A general lemma of Appendix B provides probably the simplest way, as demonstrated below.

1. $\alpha \neq \beta$. Using Green's theorem, we have for $n \geqslant 1$

$$I = \frac{n}{\hat{a}} \int_{\hat{S}_\beta} Y_{\nu\mu}(\boldsymbol{y}-\boldsymbol{x}^{\beta})\,\mathrm{d}\Omega_{\boldsymbol{y}} \int_{\hat{S}_\alpha} \tilde{G}(\boldsymbol{x},\boldsymbol{y}) \overline{Y}_{nm}(\boldsymbol{x}-\boldsymbol{x}^{\alpha})\,\mathrm{d}\Omega_{\boldsymbol{x}}, \tag{5.9}$$

where

$$\tilde{G}(\boldsymbol{x},\boldsymbol{y}) = G(\boldsymbol{y}-\boldsymbol{x}) + \tfrac{2}{3}\pi(\boldsymbol{y}-\boldsymbol{x}^{\beta})^2 + \tfrac{2}{3}\pi(\boldsymbol{x}-\boldsymbol{x}^{\alpha})^2 \tag{5.10}$$

is a harmonic function of $\boldsymbol{x}$ and $\boldsymbol{y}$. Using (B 1), the inner integral (5.9) for $m \geqslant 0$ can be written as

$$\begin{aligned} (2\hat{a})^{\nu}\left[\frac{4\pi}{(2\nu+1)!}\right]^{1/2} C_{n,m}\left[\left(\frac{\partial}{\partial x_1} - \mathrm{i}\frac{\partial}{\partial x_2}\right)^m \left(\frac{\partial}{\partial x_3}\right)^{n-m} G(\boldsymbol{y}-\boldsymbol{x})_{|\boldsymbol{x}=\boldsymbol{x}^{\alpha}} + \tfrac{4}{3}\pi\delta_{n,2}\delta_{m,0}\right] \\ = (2\hat{a})^{\nu}\left[\frac{4\pi}{(2\nu+1)!}\right]^{1/2} C_{n,m}\left\{(-1)^n\left(\frac{\partial}{\partial y_1} - \mathrm{i}\frac{\partial}{\partial y_2}\right)^m \left(\frac{\partial}{\partial y_3}\right)^{n-m} \right. \\ \left. \times\,[\tilde{G}(\boldsymbol{x}^{\alpha},\boldsymbol{y}) - \tfrac{2}{3}\pi|\boldsymbol{y}-\boldsymbol{x}^{\beta}|^2] + \tfrac{4}{3}\pi\delta_{n,2}\delta_{m,0}\right\}, \end{aligned} \tag{5.11}$$

where

$$C_{n,m} = \frac{1}{2^n}\left[\frac{(2n)!}{(n-m)!(n+m)!}\right]^{1/2}. \tag{5.12}$$

Expression (5.11) is a harmonic function of $\boldsymbol{y}$ for $n \geqslant 1$, and so the outer integral (5.9) is also calculated using the lemma of Appendix B. The result is further simplified by the identity

$$\left(\frac{\partial}{\partial y_1} + \mathrm{i}\frac{\partial}{\partial y_2}\right)\left(\frac{\partial}{\partial y_1} - \mathrm{i}\frac{\partial}{\partial y_2}\right) f = -\frac{\partial^2}{\partial y_3^2} f, \tag{5.13}$$

valid for any harmonic function $f(\boldsymbol{y})$, to a form containing the derivative

$$(D_1 \pm \mathrm{i}D_2)^{|m-\mu|} D_3^{\nu+n-|m-\mu|} G(\boldsymbol{x}), \qquad \left(D_i = \frac{\partial}{\partial x_i}\right)$$

at $\boldsymbol{x} = \boldsymbol{x}^\beta - \boldsymbol{x}^\alpha$ plus some simple additional terms.

2. $\alpha = \beta$. In this case, the normal derivative in (5.8) is understood as the limiting value from the continuous phase. Representing $G(\boldsymbol{y} - \boldsymbol{x}) = -|\boldsymbol{y} - \boldsymbol{x}|^{-1} + g(\boldsymbol{y} - \boldsymbol{x})$, one can find the contribution of the first term to (5.8) using the relation (see (B 1) and (B 3), or Hobson (1955))

$$\lim_{\boldsymbol{x} \to \hat{S}_\alpha} \frac{\partial}{\partial n_{\boldsymbol{x}}} \int_{\hat{S}_\alpha} \frac{Y_{\nu\mu}(\boldsymbol{y} - \boldsymbol{x}^\alpha)}{|\boldsymbol{y} - \boldsymbol{x}|} \, \mathrm{d}\Omega_{\boldsymbol{y}} = -\frac{4\pi(\nu+1)}{(2\nu+1)\hat{a}^2} Y_{\nu\mu}(\boldsymbol{x} - \boldsymbol{x}^\alpha) \tag{5.14}$$

and the orthogonality of spherical harmonics. The contribution of g, a regular function of $\boldsymbol{x}$ and $\boldsymbol{y}$ inside $\hat{S}_\alpha$, is calculated exactly in the same manner, as the integrals (5.8) for $\alpha \neq \beta$.

Thus, we arrive at the system of equations for $n \geqslant 1$ and $0 \leqslant m \leqslant n$:

$$U_{n,m}^\alpha = \sum_{\beta=1}^{N} \sum_{\nu=0}^{\infty} \sum_{\mu=-\nu}^{\nu} \tfrac{1}{2}(-1)^{\nu+m+1} C_{n,m} C_{n+\nu,n-\nu} C_{\nu,\mu} S_{\alpha\beta,n+\nu}^{\mu-m} U_{\nu,\mu}^\beta$$
$$+ \tfrac{4}{3}\pi\hat{a}^3 \delta_{n,1} \sum_{\beta=1}^{N} U_{1,m}^\beta + \delta_{n,1} \begin{cases} 2K_3, & m = 0 \\ \sqrt{2}(K_1 - \mathrm{i}K_2), & m = 1. \end{cases} \tag{5.15}$$

The coefficients $S_{\alpha\beta,\nu}^\mu$ for $\alpha \neq \beta$ are defined as

$$\left.\begin{aligned} S_{\alpha\beta,\nu}^\mu &= \frac{(-4\hat{a})^{\nu+1}}{2[(2\nu)!]^{1/2}} [(D_1 + \mathrm{i}D_2)^\mu D_3^{\nu-\mu} G(\boldsymbol{x})_{|\boldsymbol{x}=\boldsymbol{x}^\beta - \boldsymbol{x}^\alpha} + \tfrac{4}{3}\pi\delta_{\nu,2}\delta_{\mu,0}] \quad (\mu \geqslant 0), \\ S_{\alpha\beta,\nu}^\mu &= (-1)^\mu \overline{S_{\alpha\beta,\nu}^{-\mu}} \qquad\qquad\qquad\qquad\qquad\qquad\qquad\qquad\quad (\mu < 0). \end{aligned}\right\} \tag{5.16}$$

For $\alpha = \beta$, the relations (5.16) hold with $G(\boldsymbol{x})$ replaced by $G(\boldsymbol{x}) + |\boldsymbol{x}|^{-1}$.

In addition to (5.15), the integration of (5.3) over $\hat{S}_\alpha$ yields the equations for particle temperatures $T_1, \ldots, T_N$. To this end, the double integrals (5.9) with $n = 0$ are calculated in a similar way, resulting in

$$\frac{2}{\hat{a}}(T_\alpha - C - \boldsymbol{K} \cdot \boldsymbol{x}^\alpha) + U_{0,0}^\alpha = \sum_{\beta=1}^{N} \sum_{\nu=0}^{\infty} \sum_{\mu=-\nu}^{\nu} \frac{(-1)^{\nu+1}}{2^{\nu+1}} C_{\nu,\mu} S_{\alpha\beta,\nu}^\mu U_{\nu,\mu}^\beta, \tag{5.17}$$

where the right-hand side is a particular case of the first term in (5.15) for $n = m = 0$.

Finally, (5.15) and (5.17) are complemented by the equations (4.12) for

$$U_{0,0}^\alpha = \frac{1}{2\pi\hat{a}^2} \int_{\hat{S}_\alpha} \frac{\partial T^{\mathrm{e}}}{\partial n} \, \mathrm{d}S \tag{5.18}$$

and, in principle, uniquely determine all $U^{\alpha}_{n,m}$ and $T_1, \ldots, T_N$ (the insignificant constant C in (5.17) can be set to zero).

The average flux $\langle \boldsymbol{q} \rangle$ for the original problem can be found from (3.8) and (4.13), with

$$\int_{\hat{S}_\alpha} (\boldsymbol{x} - \boldsymbol{x}^\alpha) \frac{\partial T^{\mathrm{e}}}{\partial n} \, \mathrm{d}S = 2\pi \hat{a}^3 (\sqrt{2}\,\mathrm{Re}\, U^{\alpha}_{1,1}, -\sqrt{2}\,\mathrm{Im}\, U^{\alpha}_{1,1}, U^{\alpha}_{1,0}) \tag{5.19}$$

in the Cartesian coordinates.

The first and obvious step in the numerical solution of (4.12), (5.15), and (5.17) is the truncation

$$U^{\alpha}_{n,m} = 0 \quad \text{for } n > k_0, \tag{5.20}$$

with some $k_0 \gg 1$. For small ϵ, however, when k_0 has to be quite large, and for $N \gg 1$, the truncation (5.20) alone is extremely wasteful, since it does not take into account that only the interaction of low-order harmonics in (5.15) and (5.17) is long–ranged. A far more efficient approach of Zinchenko (1994*a*) used herein first represents the coefficients $S^{\mu}_{\alpha\beta,\nu}$ for all $\alpha \neq \beta$ in the form

$$S^{\mu}_{\alpha\beta,\nu} = \frac{1}{C_{\nu,\mu}} \left(\frac{4\pi}{2\nu+1} \right)^{1/2} \left(\frac{2\hat{a}}{|\boldsymbol{R}_{\alpha\beta}|} \right)^{\nu+1} Y_{\nu\mu}(\boldsymbol{R}_{\alpha\beta}) + (S')^{\mu}_{\alpha\beta,\nu}, \tag{5.21}$$

with $S^{\mu}_{\alpha\alpha,\nu} = (S')^{\mu}_{\alpha\alpha,\nu}$ by definition. It is known that the derivatives $D^{\nu} G(\boldsymbol{x})$ for $\nu \geqslant 3$ can be calculated as if $G(\boldsymbol{x})$ were represented by the formal sum $-\sum |\boldsymbol{x} + \boldsymbol{k}|^{-1}$, so one can easily see from (5.16) and (B3) that, for $\nu \geqslant 3$ (Zinchenko 1994*a*)

$$(S')^{\mu}_{\alpha\beta,\nu} = \frac{1}{C_{\nu,\mu}} \left(\frac{4\pi}{2\nu+1} \right)^{1/2} \sum_{\boldsymbol{k} \neq \boldsymbol{0}} \left(\frac{2\hat{a}}{|\boldsymbol{R}_{\alpha\beta} + \boldsymbol{k}|} \right)^{\nu+1} Y_{\nu\mu}(\boldsymbol{R}_{\alpha\beta} + \boldsymbol{k}) \tag{5.22}$$

and the first term in (5.21) has a sense of the nearest image contribution to the lattice sum $S^{\mu}_{\alpha\beta,\nu}$. The representation (5.21) splits the triple sum operator in (5.15) and (5.17) acting on $U^{\beta}_{\nu,\mu}$ into two, a near- and a far-field operator. The far-field operator, with $(S')^{\mu}_{\alpha\beta,\nu}$ instead of $S^{\mu}_{\alpha\beta,\nu}$, is fast converging, if there are at least several spheres in the cell V, and has to be truncated by relatively small values of n and ν. So does the near-field operator, except for close pairs $|\boldsymbol{R}_{\alpha\beta}| \approx 2\hat{a}$, when higher-order harmonics should be included. A systematic way to construct the 'economical truncation' (Zinchenko 1994*a*) is to introduce a norm in the space of $U^{\alpha}_{n,m}$ and estimate first the residual h due to the initial truncation (5.20) from the rate of convergence of the exact solution $U^{\alpha}_{n,m}$ at $n \to \infty$ (which was proved to be the same as if sphere $\hat{S}_\alpha$ were interacting only with its nearest neighbour). In the present case of superconducting spheres, a uniformly valid analytical form (derived from (B 2) of Zinchenko (1994*a*)),

$$\left[\sum_{m=-n}^{n} |U^{\alpha}_{n,m}|^2 \right]^{1/2} = O[n^{-1/2} (q_\alpha)^n] \quad \text{for } n \to \infty, \tag{5.23}$$

with

$$q_\alpha = \tfrac{1}{2}(\zeta_\alpha - (\zeta_\alpha^2 - 4)^{1/2}), \qquad \zeta_\alpha = \frac{1}{\hat{a}} \min_{\beta:\beta\neq\alpha} |\boldsymbol{R}_{\alpha\beta}|, \tag{5.24}$$

can be used to estimate h, instead of numerical solutions of two-particle problems in Zinchenko (1994*a*) (besides, in our geometry, all $q_\alpha \approx 1 - \sqrt{\epsilon}$). Next, the barrier functions $k_0^*(\alpha,\beta)$, $k_0^{**}(\alpha,\beta)$ and $\ell^{**}(\alpha,\beta)$ are constructed to restrict, for every β, the near-field summations by $n,\nu \leqslant k_0^*(\alpha,\beta)$ and the far-field summations by $n,\nu \leqslant k_0^{**}(\alpha,\beta)$ and $n+\nu \leqslant \ell^{**}(\alpha,\beta)$, so that the residuals in the near- and far-field operators after these additional truncations are still within $O(h)$. The barrier functions are calculated in exactly the same way as in Zinchenko (1994*a*) (with the constants $\chi = 5$ and $\chi = 1$ for the near- and far-field economizations, as suggested in § 3 of that paper). The lattice sums $(S')^{\mu}_{\alpha\beta,\nu}$ for the far-field operator are calculated in the Ewald-like manner for small $\nu = 4$–6 (relations (56)–(61) of Zinchenko (1994*a*)) and, when necessary, by direct summation (5.22) for higher ν, to an accuracy consistent with the residual h of the initial truncation. For different k_0, this construction results in a one-parameter family of approximations, with the convergence to the exact solution of the infinite system (4.12), (5.15), and (5.17), as $k_0 \to \infty$, since k_0^*, k_0^{**}, $\ell^{**} \to \infty$ and so all the terms in (5.15) and (5.17) are eventually included. At the same time, with practically no loss of accuracy, this economical truncation provides very large computer time savings in calculating the triple sum operator (5.15), (5.17) for $k_0 \gg 1$ and $N \gg 1$, compared to the initial truncation (5.20), since $k_0^{**} \ll k_0$, $\ell^{**} \ll 2k_0$ and also $k_0^* \ll k_0$, except for a small portion of close pairs ($|\boldsymbol{R}_{\alpha\beta}| \approx 2\hat{a}$) with $k_0^* \approx k_0$.

Another principal idea (Zinchenko 1994*a*) is to use, without any new approximations, a special 'rotational algorithm' for calculating the near-field operator, instead of direct summations (5.15) and (5.17). For any given $\beta \neq \alpha$, the near-field part of the double sum in the right-hand sides of (5.15) and (5.17) represents the action of the *invariant* operator in the coordinate form, yielding the (n,m)-Fourier coefficients of some invariant distribution on $\hat{S}_\alpha$, given the Fourier coefficients $U^{\beta}_{\nu,\mu}$ of $\partial T^{\mathrm{e}}/\partial n$ on $\hat{S}_\beta$. It is advantageous that, if the minimal vector $\boldsymbol{R}_{\alpha\beta}$ is directed along the x_3-axis, then, according to (5.4) and (5.7), $Y_{\nu\mu}(\boldsymbol{R}_{\alpha\beta}) = 0$ for $\mu \neq 0$, and so, upon substituting (5.21) into (5.15) and (5.17), only the term with $\mu = m$ contributes to the near-field operator. Thus, for every α, the near-field summations are organized as follows.

1. Initialize the

$$\binom{\alpha}{n,m}\text{-components}$$

of the near-field operator.

2. For every $\beta \neq \alpha$: (a) rotate the coordinate system (x_1,x_2,x_3) to a new position (x_1',x_2',x_3') superimposing the direction of the x_3-axis with $\boldsymbol{R}_{\alpha\beta}$; (b) calculate the Fourier coefficients $(U^{\beta}_{\nu,\mu})'$ of $\partial T^{\mathrm{e}}/\partial n$ on $\hat{S}_\beta$ in the new coordinates (θ',ϕ') (associated with x_1', x_2', x_3') via $U^{\beta}_{\nu,\mu}$ for $\nu \leqslant k_0^*(\alpha,\beta)$, using the theory of rotational transformations of spherical harmonics (theory of Wigner functions); (c) calculate the contribution of the nearest image to

$$\binom{\alpha}{n,m}\text{-components}$$

of the near-field operator in the new coordinate system (θ',ϕ') on $\hat{S}_\alpha$; (d) transform the result of operation (c) back to the initial coordinates (θ,ϕ) on $\hat{S}_\alpha$ using, again,

Wigner functions and (e) add the result of (d) to the current

$$\binom{\alpha}{n,m}\text{-components}$$

of the near-field operator.

The recurrent scheme (27) of Zinchenko (1994*a*), or the more universal relations in Appendix C of the present paper can be used for fast calculation of the Wigner functions. Most importantly, for every β, the computational cost of this algorithm is $O[(k_0^*)^3]$, compared to $O[(k_0^*)^4]$ for direct summations (5.15) and (5.17). In particular, the actual computational gain is about 10-fold for $k_0^*(\alpha,\beta)=30$.

Since (4.12), (5.15), and (5.17) are not a positive definite, self-adjoint system, we use, instead of conjugate gradient iterations (Zinchenko 1994*a*), a version of the Zeidel iterative method. Namely, given $\tilde{T}_\beta$ in (4.12) and the right-hand sides of (5.15) and (5.17), then (5.15) is used to update $U^\alpha_{n,m}$ for $n \geqslant 1$, while (4.12) and (5.17), solved simultaneously for $U^\alpha_{0,0}$ and T_α, serve to update these quantities. As the initial approximation, we set $T_\alpha = \boldsymbol{K}\cdot\boldsymbol{x}^\alpha$, $U^\alpha_{0,0}=0$ and calculate the other $U^\alpha_{n,m}$ from (5.15) with $S^{\mu-m}_{\alpha\beta,n+\nu}=0$. The convergence of the average flux vector $\langle\boldsymbol{q}\rangle$ obtained in the course of iterations is considerably improved by the familiar δ^2-transformation. As usual, the calculation of $\langle\boldsymbol{q}\rangle = -\Lambda^{\mathrm{e}}\boldsymbol{F}\cdot\boldsymbol{K}$ for three different directions of $\boldsymbol{K}$, along the coordinate axes, yields the dimensionless conductivity tensor $\boldsymbol{F}$ for a given configuration.

Both the theoretical study and numerical experiments show that this generally successful iterative scheme fails to converge when the artificial gap ϵ is below some small critical value ϵ^*. The value of ϵ^* is roughly $35/\gamma^2$ for the case $\rho_{\alpha\beta}=0$, and smaller for a granular material with contact deformations. In our calculations for $\epsilon<\epsilon^*$, it was always possible to find the solution by a slightly different iterative technique (and the results match those for $\epsilon>\epsilon^*$, in support of the statement in § 3 that (3.14) (or (4.12)) is a well-posed problem for all $\epsilon>0$). Namely, T_α is updated directly from (5.17), and $U^\alpha_{0,0}$ from (4.12) with underrelaxation. The relaxation parameter has to be determined experimentally in the course of iterations, making this scheme much less convenient. Fortunately, the existence of ϵ^* is not a serious limitation, since we are mostly interested in large values of γ, when ϵ^* is quite small and the limit $\epsilon\to 0$ can be accurately estimated for ϵ well above ϵ^*.

Obviously, an increasing number of harmonics is required for $\epsilon\to 0$, and so we used $k_0\approx(3\text{–}4.5)\epsilon^{-1/2}$ in our calculations of § 6, the $\epsilon^{-1/2}$-dependence being prompted by (5.23)–(5.24). The absolute difference in the elements F_{ij} of the conductivity tensor calculated for $k_0\approx 3\epsilon^{-1/2}$ and $k_0\approx 4.5\epsilon^{-1/2}$ was found to be within 0.016, independent of γ, Π, and a configuration. Finally, the number of iterations for F_{ij} to converge with the absolute accuracy of 10^{-3} is roughly $1.5\epsilon^{-1/2}$ for $\epsilon^*<\epsilon\ll 1$ and ϵ not very close to ϵ^*.

6. Numerical results

First, it is interesting to explore how easily the limit $\epsilon\to 0$ can be achieved in our conductivity simulations. Figure 7*a*, *b* presents the dimensionless effective conductivity along the x_1-axis versus ϵ, both for a small random close packing ($N=20$) with $\gamma=200$ and point contacts ($\Pi=0$), and for a relatively large RCP configuration ($N=100$) with $\gamma=340$ and contact deformations ($\Pi=0.01$). Crosses

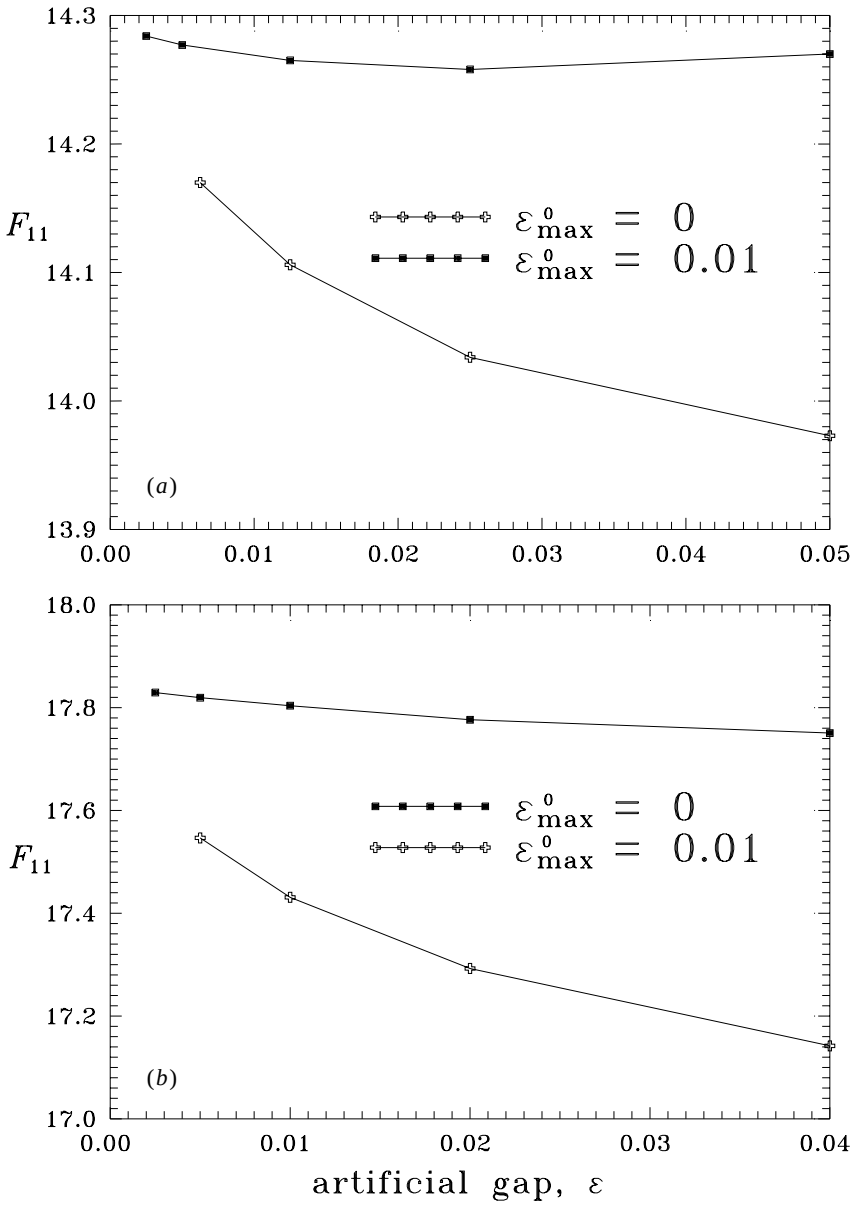

Figure 7. The sensitivity of the effective conductivity by the semi-asymptotic theory to the artificial gap between the spheres. (*a*) $N = 20$, $c = 0.634$, $\gamma = 200$, $\Pi = 0$; (*b*) $N = 100$, $c = 0.628$, $\gamma = 340$, $\Pi = 0.01$

represent the solution with the consistency conditions in the original form (3.14) and (3.17), squares—with near-neighbours included, as suggested in (4.12)–(4.13) (for $\epsilon^0_{\max} = 0.01$). Of course, when $\epsilon \to 0$, both the solutions tend to the same limit, but the convergence is much faster when near-neighbours are accounted for. The choice $\epsilon^0_{\max} = 0.01$ was also found to provide similar fast convergence, when $\epsilon \to 0$, for the other packings with different γ and Π.

PHILOSOPHICAL TRANSACTIONS OF THE ROYAL SOCIETY A MATHEMATICAL, PHYSICAL & ENGINEERING SCIENCES

According to the strategy of § 3, this limit $\epsilon \to 0$ corresponds to the solution for touching particles of *finite* conductivity by matched asymptotic expansions, valid for $\gamma \gg 1$ and $\Pi \ll 1$, and the basic question is how accurate our semi-asymptotic theory itself is. Fortunately, it has proved possible, for comparison, to calculate exactly the conductivity of several small random close packings with *point* contacts and γ up to several hundred, using the algorithm of Zinchenko (1994*a*) developed for *arbitrary* γ. This code was verified previously by the comparison with McPhedran & McKenzie's (1978) calculations for a simple cubic array of superconducting spheres near close packing and with boundary-integral calculations for a small random array of well-mixed non-touching spheres at the volume fraction $c = 0.5$ and $\gamma = 20$ (Zinchenko 1994*a*). The one, but very important, difference is a new, absolutely stable method of calculating the Wigner functions (Appendix C) we used in the rotational part of that algorithm. The recurrent relations (27) of Zinchenko (1994*a*) were observed to lose numerical stability for the harmonic order $\ell \geqslant 110$–115, whereas the present calculations required much higher values of ℓ, because of the extremely slow convergence for high γ. The extrapolation $k_0 \to \infty$ to the exact solution, necessary for large γ, is somewhat intricate and has been found to be linear in

$$k_0^{-1} \exp\left[-2\left(k_0 \ln \frac{\gamma+1}{\gamma-1}\right)^{1/2}\right], \tag{6.1}$$

where the exponential factor is prompted by the analytical result (B3) of Zinchenko (1994*a*) for the rate of decay of Fourier coefficients in a system of touching spheres of finite conductivity. Figure 8 demonstrates the dependence of F_{11} on k_0 for one random close packing with $N = 9$ (untypically small RCP density 0.582 in this case is due to larger dispersion for small N) and different γ, up to 600. For very high k_0, the convergence should be faster than in figure 8, due to extremely small, but non-zero gaps between nominal neighbours in computer-generated packings (§ 4). The effect of gaps on the rate of decay of Fourier coefficients is described by exponents $(q_\alpha)^n$ (see (5.23)–(5.24), with $\hat{a}$ replaced by a) and so, for $\zeta_\alpha \approx 2$, the error in the conductivity is believed to be reduced approximately by a factor $\exp[-k_0(\overline{\zeta}-2)^{1/2}]$, where $\overline{\zeta}$ is the average of ζ_α. For this packing, $\overline{\zeta} - 2 = 1.6 \times 10^{-8}$, and so the effect of gaps on the rate of convergence could be significant only for $k_0 \gg 1000$, when the conductivity is already very close to the exact solution. For this reason, a linear extrapolation of the data in figure 8, as shown by dashed lines, is permissible as a very accurate estimation of the exact solution for high γ. For $\gamma \leqslant 200$ (not shown in figure 8), we used $k_0 \leqslant 180$ and, when necessary, the same extrapolation to obtain exact results. This exact solution, although successful, is very time-consuming, when γ is large, even for a small number $N = 9$ of spheres used. For example, when $\gamma = 600$ and $k_0 = 470$, the calculation took 45 iterations and about 10 h on an IBM AIX RISC/6000 workstation. Without the ideas of rotational transformations and economical truncation, the essence of the algorithm, the solution in this case would be about 240 times slower and intractable.

In contrast, the semi-asymptotic solution for this configuration and different γ was found relatively easily, with the absolute error about 0.003 in F_{11}, using $\epsilon = 0.0125$ and $k_0 = 40$. Unlike in the exact calculations, no computational difficulties appear when γ grows; conversely, the number of iterations slightly decreases. Since the exact solution has been obtained for slightly non-touching spheres, the existence of these

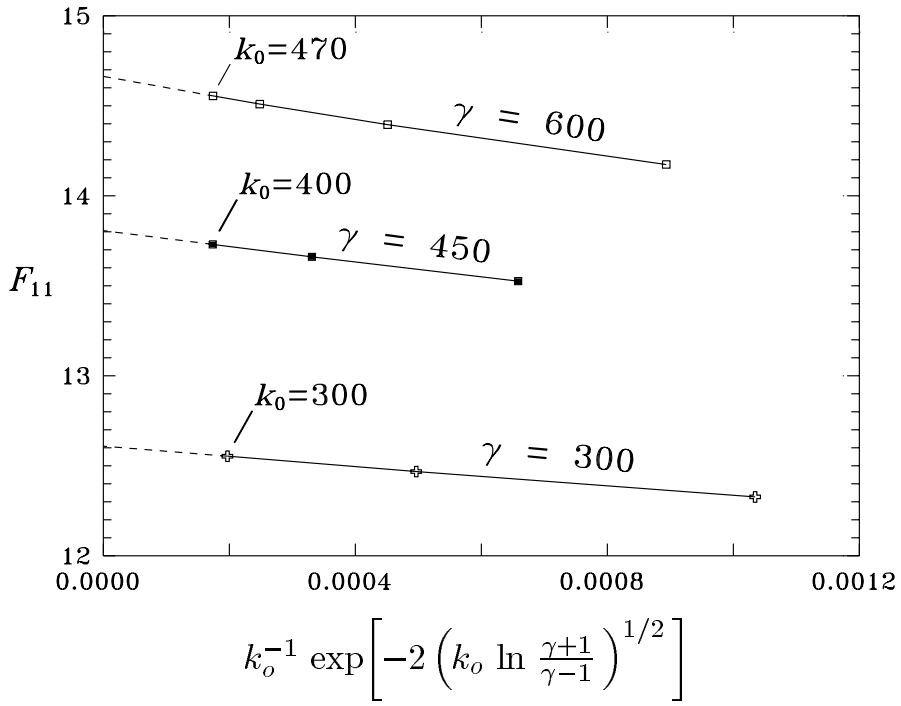

Figure 8. The dependence of the effective conductivity F_{11} along the x_1-axis on the maximum order of harmonics retained, k_0, for a random close packing with $N = 9$, $c = 0.582$ and point contacts. These numerical data are obtained by Zinchenko's (1994*a*) algorithm, and the extrapolation $k_0 \to \infty$ (dashed lines) corresponds to the exact solution.

extremely small gaps between nominal neighbours was also accounted for in the semi-asymptotic solution, by taking $\Psi_{\alpha\beta} = \ln\gamma^2 - 3.927 - \gamma^2\epsilon^0_{\alpha\beta}/12$ (see (2.27)). However, the gap corrections $-\gamma^2\epsilon^0_{\alpha\beta}/12$ were found to reduce F_{11} only by about 0.004 even for $\gamma = 600$, due to the very high degree of contactness (the average gap between nominal neighbours being $\approx 10^{-7}a$). Figure 9 demonstrates remarkable agreement between the exact and the semi-asymptotic solutions for all $\gamma \geqslant 70$, the relative error for $\gamma \geqslant 100$ not exceeding 0.9%. The absolute error reaches a maximum at γ about 450, and then decreases. We believe that the excellent accuracy of our semi-asymptotic theory for all $\gamma \geqslant 70$ is due to the fact that $\ln\gamma$ is taken as a finite parameter, and so the outer temperatures $T_1, \ldots, T_N$ depend on γ. We could act differently and rigorously expand the solution (for $\rho_{\alpha\beta} = 0$) in $\ln\gamma$, assuming $\ln\gamma \gg 1$. As follows from (3.6)–(3.7), the outer temperatures, to the leading order, satisfy

$$\sum_{\beta\in\mathcal{A}_\alpha} (\tilde{T}_\beta - T_\alpha) = 0 \tag{6.2}$$

independently of γ and are easily determined from (6.2) by relaxation techniques. These temperatures can be used, in principle, to solve the outer problem for touching superconductors and calculate the flux defects Q_α. These defects further determine $O(|\ln\gamma|^{-1})$-corrections to the outer temperatures from (3.6)–(3.7) and so on. The expansion of the conductivity in $\ln\gamma$ is found from (3.8) and (3.10). In practice, this process is applied to the consistency conditions (3.14) and (3.17), or (4.12)–(4.13),

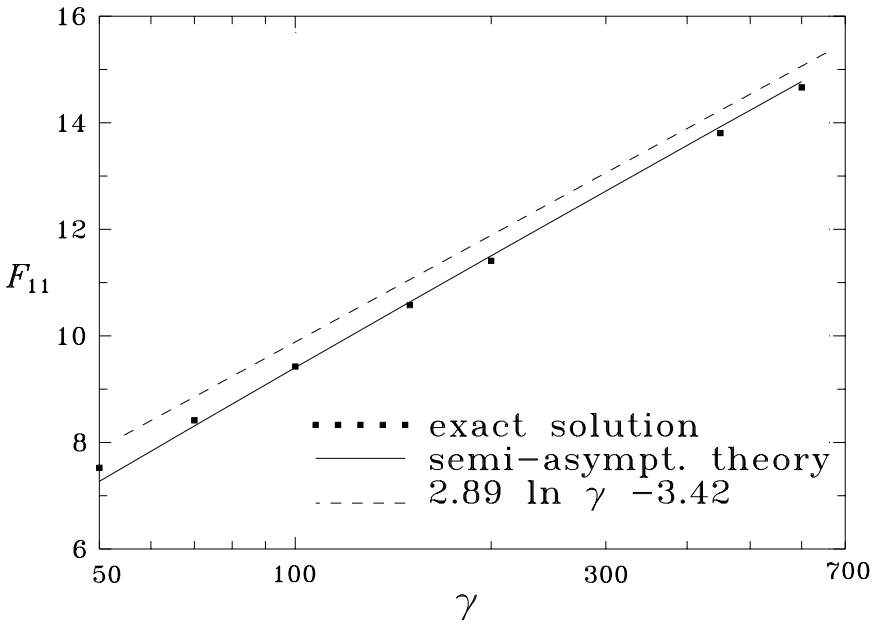

Figure 9. Comparison of exact and approximate conductivities F_{11} for a random close packing with $N = 9$, $c = 0.582$ and point contacts. The dashed line is the two-term asymptotic expansion in $\ln\gamma$ for $\gamma \to \infty$.

before the limit $\epsilon \to 0$ is taken. In this manner, the two-term expansion of F_{11} in $\ln\gamma$ for the given configuration was found (the dashed line in figure 9). Compared to the semi-asymptotic solution, this procedure is not simpler (since the outer problem also has to be solved) and proves to be much less accurate. The accuracy of this approach cannot be easily improved by calculating further terms, because an expansion in inverse powers of $\ln\gamma$ is computationally inefficient. Even though the semi-asymptotic graph in figure 9 is almost straight in $\ln\gamma$, the parameters of the best linear fit in the practical range $\gamma \leqslant O(10^3)$ are not close to those in the hypothetical limit of $\ln\gamma \to \infty$. Figure 10 confirms that some of the outer temperatures calculated by the semi-asymptotic theory, indeed, approach their limiting values, determined by (6.2), quite slowly, as $\gamma \to \infty$.

The configuration for figure 9 was chosen not to contain close non-neighbours (near-neighbours); more specifically, the minimum gap between non-neighbours in this configuration is $0.05a$. The presence of near-neighbours in more typical random close packings should make the semi-asymptotic theory somewhat less accurate. Indeed, the gaps between non-neighbours are treated in our theory as the gaps between superconductors, thus overestimating the actual local flux. We believe this is the main reason for slight overestimation of the conductivity by the semi-asymptotic solution for large γ, but there is no rigorous way to account for this and modify our theory. The comparison of the exact and semi-asymptotic solutions for larger and typical random close packings ($N = 20$ and 50) is given in figure $11a, b$. Exact results were obtained by computationally very intensive calculations using $k_0 \leqslant 400$ for $N = 20$ and $k_0 \leqslant 300$ for $N = 50$, with the extrapolation $k_0 \to \infty$ when necessary, as in figure 8. Again, the very small gaps between nominal neighbours (with

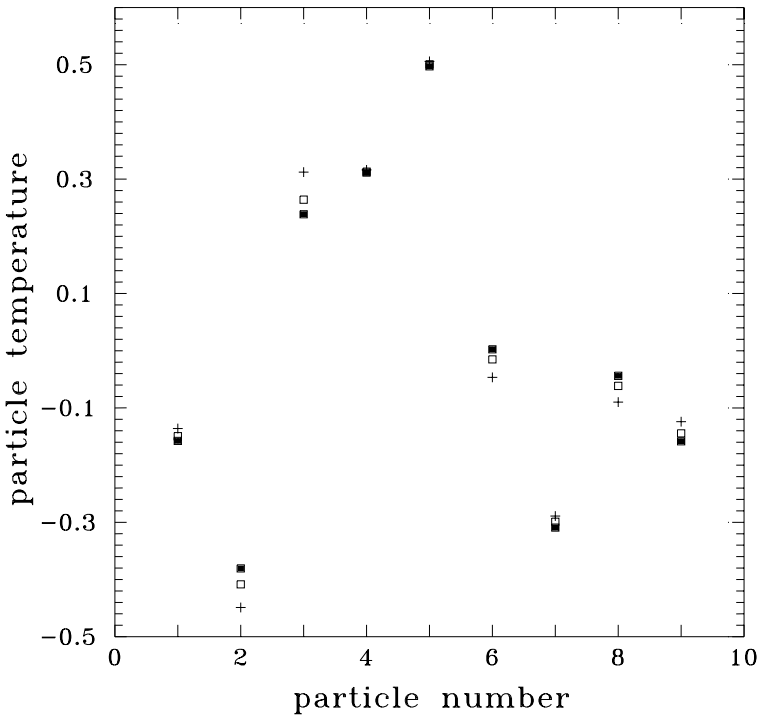

Figure 10. The particle temperatures, T_α, by the semi-asymptotic theory for a random close packing with $N = 9$, $c = 0.582$ and point contacts. Dark squares are for $\gamma = 80$, light squares for $\gamma = 600$, and crosses for $\gamma \to \infty$. In each case, the average particle temperature in the periodic cell is made zero, by adding a suitable constant to all T_α.

the average $3 \times 10^{-7}a$ for $N = 20$ and $10^{-7}a$ for $N = 50$) have no appreciable effect on the conductivity simulations by the semi-asymptotic theory in the studied range $\gamma \leqslant 400$, nor do they affect the extrapolation $k_0 \to \infty$ in the exact calculations. The absolute difference between the two solutions reaches a maximum (0.26 for $N = 20$ and 0.29 for $N = 50$) at some large $\gamma \sim 200$ and then slightly decreases. Presumably, the studied range $\gamma \leqslant 400$ is insufficient to observe further substantial decrease of the absolute error, which is expected to behave like $O(\gamma^{-1})$ (with some fairly large coefficient, see below) at $\gamma \to \infty$. The relative error drops from 2.6% for $\gamma = 100$ to 1.9% for $\gamma = 300$, when $N = 50$; for $N = 20$, the error is within 1.8% in the whole range $\gamma \geqslant 80$. Although these errors are higher than in figure 9, our semi-asymptotic solution is still quite successful and much more accurate than the two-term asymptotic expansion in $\ln\gamma$ (the dashed line in figure 11*b*). Moreover, since the statistics of near-neighbours in the packing with $N = 50$ is already close to that for $N = 100$ and 200 (figure 12), the error of the semi-asymptotic theory for large random close packings with $\gamma = O(10^2$–$10^3)$ is also expected to be about 2–2.5%. The applicability of our theory to large packings can be also explained by the fact that the finite γ-correction $P(\gamma^2\epsilon_{\alpha\beta})$ to the local flux between near-neighbours (see (2.8)) behaves like $\pi^2/(\gamma\epsilon_{\alpha\beta}^{1/2})$ for $\gamma\epsilon_{\alpha\beta}^{1/2} \gg 1$, as follows from (2.24), and the integrable singularity $\epsilon_{\alpha\beta}^{-1/2}$ for small gaps makes the overall $O(\gamma^{-1})$-correction fairly large, but finite. Note that the alternative of exact calculations for large packings and $\gamma \sim O(10^3)$ would be very prohibitive.

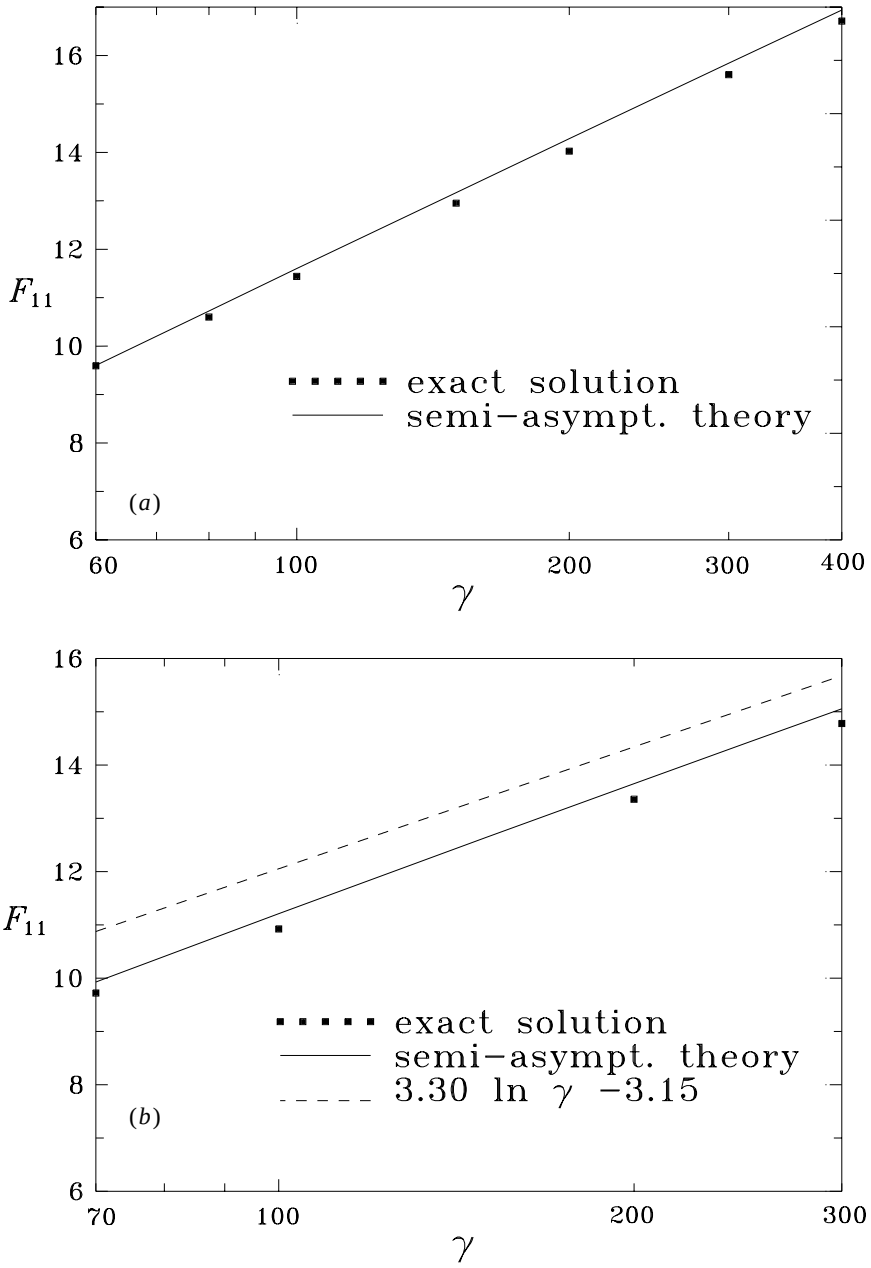

Figure 11. Comparison of exact and approximate conductivities F_{11} for typical random close packings of non-deformed spheres with (*a*) $N = 20$, $c = 0.634$ and (*b*) $N = 50$, $c = 0.618$. The dashed line in figure 11*b* is the two-term asymptotic expansion in $\ln\gamma$ for $\gamma \to \infty$.

It should not be surprising that our exact value of $F_{11} = 16.71$ for $\gamma = 400$ and $c = 0.634$ from figure 11*a* exceeds the maximum conductivity of 15.03 calculated so far for a body-centred cubic (BCC) lattice of superconducting spheres at the volume fraction of $c = 0.677$, very close to the maximum packing value of $c_{\max} = \sqrt{3}\pi/8$

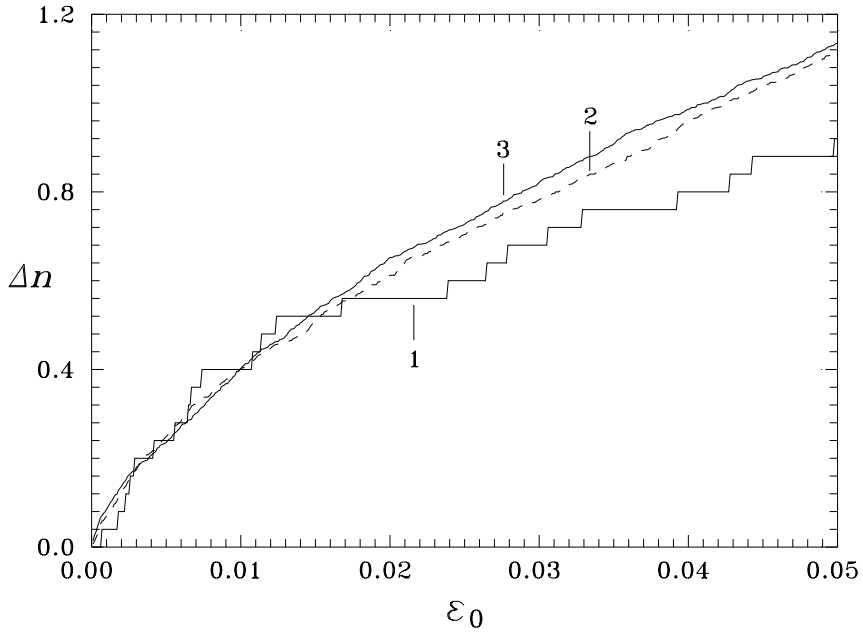

Figure 12. Average number Δn of near-neighbours of a sphere in a random close packing, within the centre-to-centre distance $a(2+\epsilon_0)$. Line 1 is for an individual packing with $N = 50$ (the same configuration as in figure 11*b*); lines 2 and 3 are averages over 15 and 10 packings with $N = 100$ and 200, respectively.

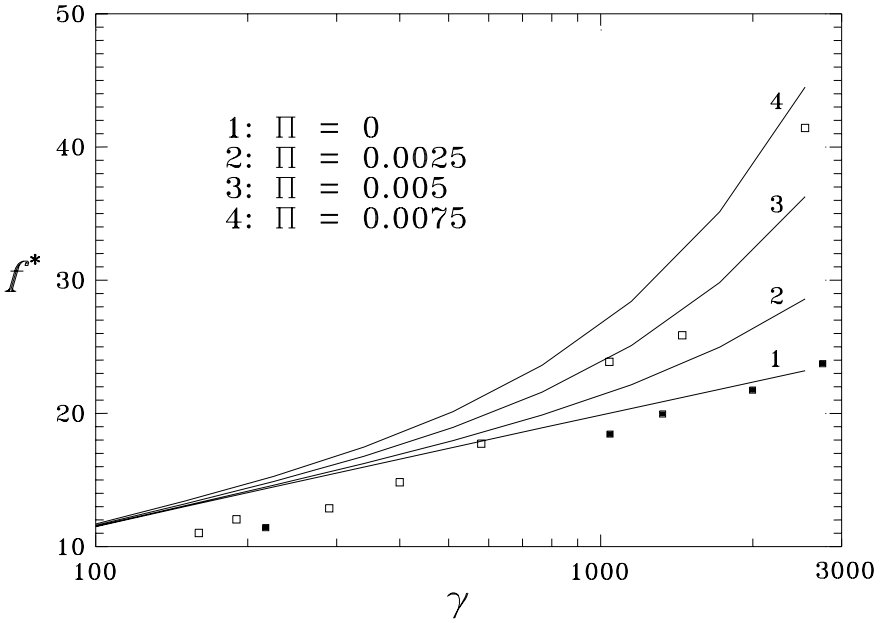

Figure 13. Effective conductivity f^* of randomly packed granular materials versus the conductivity ratio. Lines 1–4 are from the present semi-asymptotic theory (table 3), and the light and dark squares are experimental data of Turner (1973) and Kling (1938), respectively.

Table 3. *Effective conductivity f^* of random close-packed granular materials with contact deformations* ($N = 200$)

Π	$\gamma = 100$	150	225	340	510	765	1150	1721	2540
0	11.49	12.99	14.48	15.98	17.45	18.91	20.37	21.81	23.20
0.0025	11.52	13.06	14.61	16.24	17.95	19.87	22.15	24.98	28.59
0.005	11.60	13.20	14.89	16.78	18.94	21.59	25.09	29.83	36.27
0.0075	11.70	13.41	15.27	17.47	20.13	23.61	28.41	35.14	44.50
0.01	11.83	13.65	15.71	18.25	21.45	25.79	31.93	40.69	53.00
0.015	12.15	14.23	16.72	19.98	24.33	30.43	39.30	52.16	70.40
0.02	12.52	14.88	17.85	21.87	27.39	35.29	46.92	63.92	88.13

Table 4. *Effective conductivity f^* of random close-packed granular materials with contact deformations* ($N = 100$)

Π	$\gamma = 100$	225	510	1150	1721
0	11.42	14.38	17.32	20.22	21.65
0.005	11.52	14.79	18.80	24.89	29.57
0.01	11.75	15.60	21.29	31.64	40.31
0.02	12.43	17.71	27.15	46.46	63.27

Table 5. *Effective conductivity f^* of random close-packed granular materials with point contacts*

$\gamma = 2$	3.5	5	7.5	10	14	20	30	45	70
1.56	2.25	2.81	3.59	4.22	5.04	6.01	7.21	8.49	9.97

(McKenzie *et al*. 1978). The volume fraction and the coordination number in our case are smaller, but the local flux between two touching spheres with $\gamma = 400$ turns out to be higher than that between superconducting spheres in the BCC lattice at $c = 0.677$. Indeed, the non-dimensional gap ϵ in the latter case is 0.00312, and so the local flux (3.12) between superconducting spheres contains $\ln(\epsilon^{-1}) = 5.77$, compared to $\ln 400^2 - 3.927 = 8.06$ in (2.28) for touching spheres with $\gamma = 400$.

In the practical case of a random granular material with contact deformations, there seems to be no prospect of exact conductivity simulations at all even for small N, at least with $\gamma \sim O(10^3)$ and typically small contact spot radii. Our semi-asymptotic theory, however, that has proved successful for materials with point contacts, can be also used with confidence as a very accurate approximate method to account for contact deformations. The only computational difference is the full expression (3.7) to be used for $\Psi_{\alpha\beta}$. It should be clearly understood that the contact deformations do not contradict the existence of (extremely) small gaps between neighbours in our computer-generated packings; these configurations are used only to approximate the outer geometry of perfectly touching spheres with point contacts, and the actual gaps between neighbours are insignificant, since they are much smaller than the values of ϵ necessary for convergence $\epsilon \to 0$. Table 3, the main result of the present work, presents the dimensionless effective conductivity f^* of a random close-packed granular material as a universal function of the two parameters, $\gamma \gg 1$

and the elastic parameter $\Pi \ll 1$. These results are obtained by averaging over 10 packings with $N = 200$ (average density 0.631), the conductivity f^* being defined for each configuration as $(F_{11} + F_{22} + F_{33})/3$; small off-diagonal elements F_{ij} disappear on averaging and are of no interest. The boundary-value problem was solved three times for each configuration, with $\epsilon = 0.005$, $\epsilon^0_{\max} = 0.01$, $k_0 = 40$, and some 3×20 iterations, each iteration taking about 23 s on an IBM AIX RISC/6000 workstation; in this case, the total computational gain through the economical truncation and the rotational algorithm is about 320-fold. The statistical error of the values in table 3, estimated through the data dispersion, as usual, is 0.2–0.3%, i.e. less than the expected error of the semi-asymptotic theory itself. To explore the effect of the particle number, calculations have been also performed for $N = 100$ and several selected pairs (γ, Π), with averaging over 15 random close packings (table 4, the average packing density 0.628). The difference between the results for $N = 100$ and 200 is systematic, but only 0.7–1%. For one of the configurations with $N = 100$, $\gamma = 340$, $\Pi = 0.01$, we checked the accuracy of the solution of the boundary-value problem (the difference in f^* for $k_0 = 40$ and 60 being only 0.016) and found $\epsilon = 0.005$ sufficient to estimate the limiting value of f^* at $\epsilon \to 0$ to about 0.01 (figure 7*b*).

These numerical results can be complemented by two simple cases when the solution of the boundary-value problem is not required. The first is the case of non-deformed spheres with extremely high γ, when

$$f^* \sim 3.51 \ln \gamma. \tag{6.3}$$

The coefficient 3.51 here is obtained through the numerical solution of (6.2), as the slopes of dashed lines in figures 9 and 11*b*, and represents the average over 10 packings with $N = 200$ (averaging over 15 RCP configurations with $N = 100$ yields a close value 3.48). The analytical theory of Batchelor & O'Brien (1977) gives the somewhat different value 4.0, because their 'effective' coordination number 6.5 (instead of 6) and approximate averaging both lead to slight overestimation. We did not proceed with calculating further terms in (6.3), since this approach was shown for individual configurations to be less accurate than the semi-asymptotic solution.

The second is the case of 'vacuum environment', when the conduction is only through the small contact spots. In this case the flux between neighbours is

$$2\gamma \Lambda^{\mathrm{e}} \rho_{\alpha\beta} (\tilde{T}_\beta - T_\alpha)$$

(Yovanovich 1975; Batchelor & O'Brien 1977), and so the flux balance equations take the form

$$\sum_{\beta \in \mathcal{A}_\alpha} \rho_{\alpha\beta} (\tilde{T}_\beta - T_\alpha) = 0, \tag{6.4}$$

the mechanical load only affecting the proportionality factor in $\rho_{\alpha\beta}$. The outer temperatures $T_1, \ldots, T_N$ are determined numerically from (6.4) and used to find the contact spot contributions to the average flux, resulting in a simple relation

$$f^* \sim 1.46 \gamma \Pi. \tag{6.5}$$

The coefficient 1.46 is the average over 10 packings with $N = 200$ (compared to 1.45 for averaging over 15 configurations with $N = 100$). Previously, the vacuum-environment conductivity was rigorously determined only for different regular packings, when the solution of (6.4) is not required (Chan & Tien 1973), and these results,

sensitive to the packing type, cannot be used for comparison. Obviously, (6.5) is an approximation to $f^*(\gamma, \Pi)$ for $\Pi \neq 0$ and $\gamma \to \infty$, but, in practice, γ has to be very large for (6.5) to be valid. For example, (6.5) underestimates f^* by a factor of about two, when $\gamma \sim 1000$ and $\Pi = 0.01$; the error of (6.5) for $\Pi = 0.02$ and $\gamma = 1721$ is still 21%.

Figure 13 demonstrates the effect of contact deformations on the conductivity of granular materials. To give some idea of how noticeable this effect can be under normal conditions, we note that for a free-standing (without external load) bed of relatively rigid steel balls in a gas, the elastic parameter Π is about 0.005 at the depth of 50 cm below the surface, and for a typical value $\gamma = 1150$ our theory predicts $f^* = 25.1$ compared to 20.4 for non-deformable particles; with an additional load of 170 kPa, f^* further increases to 31.9. The deformation effect can be much more pronounced for softer, non-metallic particles.

On the other hand, table 3 shows that, for $\gamma < 100$, which is often the case for liquid-particle systems, the deformation effect is small under most practical situations, and so we have complemented tables 3 and 4 by the values of f^* for random close-packed granular materials with point contacts and small-to-moderate conductivity ratio γ (table 5). These numerical data are obtained using the exact algorithm of Zinchenko (1994*a*) and are averages over 15 packings with $N = 100$. Different values of $k_0 \leqslant 100$ were used for each γ, to ensure an absolute accuracy of f^* within 0.01 for a typical configuration. The convergence $k_0 \to \infty$, although much better than in figure 8, is still slow for moderately high γ due to the interparticle contacts; e.g. for $k_0 = 10$ the conductivity f^* is 9% in error, when $\gamma = 45$. A new strategy (Sangani & Mo 1994) has been recently proposed to bypass using high-order harmonics (or multipoles) in the solution of boundary-value problems of suspension hydrodynamics. However, to the best of our knowledge, this approach has not been tested yet in granular media conductivity simulations. As expected, for small $\gamma \leqslant 2$, the Maxwell–Clausius–Mosotti approximation $f^* = [\gamma + 2 + 2(\gamma - 1)c][\gamma + 2 - (\gamma - 1)c]^{-1}$, with $c = 0.628$ as the average density for $N = 100$, is very accurate.

7. Comparison with experiments

In contrast to contact deformations always increasing the conductivity, there are several practical factors ignored in our analysis that act in the opposite direction: (1) interparticle friction, (2) container-size effects, and (3) additional thermal resistance due to surface roughness in the contact areas. Highly frictional particles having been poured into a large vessel are known to form a random 'loose' packing and shrink to a random close packing only after considerable shaking or vibration (Scott & Kilgour 1969). Both the loose packing density, which can be as low as 0.56–0.57 (Scott & Kilgour 1969; Onoda & Liniger 1990), and, most importantly, a reduced number of contacts can make the experimental conductivities lower than for idealized random close packings. (It is also true that the friction may have some effect on the contact radii in experimental random close packings prepared by vibration, making the problem of finding the contact forces statically indeterminate. However, regardless of how this difficult indeterminacy is resolved, this effect is believed to be very small for small friction coefficients, due to the 1/3-exponent in (4.8).) Second, the experimental random close-packing densities are somewhat sensitive to finite particle-to-box size ratios $2a/L$ (e.g. according to Scott & Kilgour (1969), the experimental density

can be 3.5–4% lower for $2a/L = 0.1$ than in the limit $a/L \to 0$). This should also have some effect on the conductivity, unless a proper extrapolation is made. Unfortunately, we cannot estimate the effect of surface roughness in the contact areas on granular media conductivity, because the existing experiments on contact conductance are irrelevant (as discussed in § 1), but this effect is expected to be typically small, due to large contact pressures (see § 1).

At present, an adequate comparison of our theoretical calculations given in tables 3–5 with experimental data meets some difficulties, because the available experiments emphasized the effect of γ on f^*, and the other factors affecting the conductivity were not controlled, leading to some random scatter of experimental points (Batchelor & O'Brien 1977, fig. 6). More recently, Duncan *et al.* (1989) claimed to have studied systematically the effect of a mechanical load on the granular media conductivity, but their results look confusing even for free-standing packed beds. For example, at zero external load, the effective conductivity of a granular material with steel balls in nitrogen and argon environments under atmospheric pressure was found to be about 5.6 and 5 $\mathrm{W\,m^{-1}\,K^{-1}}$, respectively (fig. 3c of their paper). From these data, we find $f^* = 190$–250 for $\gamma = 530$–790, using the conductivities $\Lambda^{\mathrm{e}} = 0.029$ and 0.020 $\mathrm{W\,m^{-1}\,K^{-1}}$ for nitrogen and argon, respectively, at the average bed temperature 338 K (Song *et al.* 1993). These values of f^* are an order of magnitude higher than the data of several other authors (fig. 6 of Batchelor & O'Brien) who also experimented with steel balls in various gases, the discrepancy far exceeding the typical scatter of effective conductivity measurements. Besides, Duncan *et al.* (1989) do not explain why their free-standing bed conductivity is unchanged, when the steel balls are replaced by aluminium particles an order of magnitude more conductive, both for gaseous and vacuum environments. We believe there may be a measurement error or some strong, non-controlled factor, making these experiments unsuitable for comparison.

Among the other data, we have chosen Turner's (1973) and Kling's (1938) measurements (figure 13) as the least sensitive to container-size effects. Turner's data (light squares) are for electrical conductivity of packed beds of relatively soft ion-exchange resin balls (bed height 10 cm, particle diameter 0.5–1 mm, packing density 0.60) in aqueous solutions of NaCl, while Kling's measurements (dark squares), taken from Batchelor & O'Brien (1977), are for the effective thermal conductivity of steel balls in various gases at a packing density 0.62. Unfortunately, the specific gravity of Turner's particles is known only approximately ($\Delta\rho > 0.1\ \mathrm{g\,cm^{-3}}$), and the elastic modulus of ion-exchange resin was unavailable from the literature, and so even a rough estimate of the average elastic parameter Π for his experiments can not be made. However, a strong increase of f^*, nonlinear in $\ln\gamma$, can be only explained by particle deformations in Turner's experiments. Kling's measurements should be less affected by deformations, but the bed height in his experiments was unavailable to find the average elastic parameter Π. For small $\gamma \sim 100$, when the deformation effect is weak, both Turner's and Kling's experimental data are slightly below the theoretical values, and these differences are most likely due to the friction effect, not to the additional contact resistance. When the experimental data on the contact conductance between rough surfaces at high contact pressures become available, our theory can be very simply modified. Namely, if the asperity size is small compared to $\rho_{\alpha\beta}$, the temperature continuity at the circle of contact (2.32) can be replaced by an empirical correlation, relating the temperature jump to the thermal flux den-

sity, local pressure, surface morphology and, perhaps, some other parameters. Thus, (2.29) can be solved anew to determine $H_c + \Delta H_m$, leaving all the rest of our method and numerical codes unchanged. As for the friction effect, probably, the most important correction to our theory, it seems promising to use in future calculations a novel quasi-static approach to simulating granular assemblages of frictional particles (Goddard *et al*. 1993, 1994) in a combination with our methods for solving boundary-value problems.

8. Conclusions and future work

A novel simulation method capable of calculating the effective conductivity of randomly packed granular materials with high particle-to-medium conductivity ratio γ has been developed. The basic element is the highly efficient strategy for solving the multiparticle boundary-value problem by matched asymptotic expansions for $\gamma \gg 1$. We neglect the $O(\gamma^{-1})$ corrections due to the particle temperature non-uniformity in the outer region, but take $\ln\gamma$ as a finite parameter, and so the outer problem for touching superconductors is coupled to the near-contact solutions; in the latter, small contact deformations under a mechanical load are accounted for. Contact spot radii are rigorously found as perturbations from the Hertz theory and the mechanical balance of normal contact reactions on the microscale. Using this method, the non-dimensional effective conductivity for random close-packed beds of smooth uniform spheres is found by large-scale simulations, as a universal function of γ and the non-dimensional average pressure in the material. High accuracy (1–2.5%) of our asymptotic approach for all $\gamma \geqslant 100$ is demonstrated by the comparison with the exact solution for several individual small-to-moderately large packings of non-deformed spheres. Due to some idealizations in the analysis, a future experimental check of the present theory would require conductivity measurements for carefully prepared random close packings of low-friction spheres, like those in the experiments of Scott & Kilgour (1969). On the other hand, the present calculations can be easily generalized to include the additional contact resistance due to surface roughness in the contact areas, when the relevant experimental data for two particles become available. Besides, it seems possible to include frictional effects in future conductivity simulations, using recent advances in granular mechanics (Goddard *et al*. 1993, 1994) and our methods for solving the boundary-value problem.

Apart from static granular materials, a promising application of our methodology is a *dynamic* simulation of flowing suspensions at extremely high volume fractions, close to the 'percolation-like threshold', when large clusters of nearly touching particles should form (as was first discovered in model two-dimensional simulations by Brady & Bossis (1984) and Bossis & Brady (1985)). Even though the main term in the lubrication resistance between solid spheres is strongly singular, $O(\epsilon^{-1})$, there is no evidence, either from experiments or theoretical works, that this term solely determines the singularity of the bulk properties of random flowing suspensions at extreme volume fractions; otherwise, the observed suspension viscosities would have been much higher. Thus, the logarithmic term, $\ln\epsilon^{-1}$, is also of vital importance, and $O(1)$-contributions from the outer region cannot be neglected as well. This makes the problem close to that of granular media conductivity, although the structure ('coordination number', etc.) will be different. On these grounds, it seems possible to develop an adequate simulation method for extreme volume fractions in the spirit

of matched asymptotic expansions of § 3, with explicit lubrication terms, not based on pairwise additivity approximations.

I am grateful to Professor R. H. Davis for encouraging support and helpful discussions.

Appendix A. The analysis of a model two-sphere problem

A standard bispherical coordinate solution for two equal perfectly conducting spheres $\hat{S}_\alpha$ and $\hat{S}_\beta$ of radius $\hat{a}$ kept at temperatures T_α and T_β in an unbounded medium ($T \to 0$ at infinity) yields the expressions for the flux

$$\frac{1}{\hat{a}} \int_{\hat{S}_\alpha} \frac{\partial T^{\mathrm{e}}}{\partial n} \, \mathrm{d}S = -2\pi \sinh \eta_0 \sum_{n=0}^{\infty} \left[\frac{(T_\alpha + T_\beta)\mathrm{e}^{-(n+1/2)\eta_0}}{\cosh(n+1/2)\eta_0} + \frac{(T_\alpha - T_\beta)\mathrm{e}^{-(n+1/2)\eta_0}}{\sinh(n+1/2)\eta_0} \right] \tag{A 1}$$

and the thermal dipole

$$\frac{1}{\hat{a}^2} \int_{\hat{S}_\alpha} (z - z^\alpha) \frac{\partial T^{\mathrm{e}}}{\partial n} \, \mathrm{d}S = 2\pi \sinh \eta_0 \sum_{n=0}^{\infty} \mathrm{e}^{-(2n+1)\eta_0} [\cosh \eta_0 - (2n+1) \sinh \eta_0] \times [(T_\alpha + T_\beta) \tanh(n + \tfrac{1}{2})\eta_0 + (T_\alpha - T_\beta) \coth(n + \tfrac{1}{2})\eta_0], \tag{A 2}$$

where $\cosh \eta_0 = 1 + \epsilon/2$ and $\epsilon\hat{a}$ is the gap between the spheres. Using the Euler–McLauren formula (e.g. Abramowitz & Stegun 1964), one can derive the asymptotic relation

$$h \sum_{n=o}^{\infty} f[(n + \tfrac{1}{2})h] \sim \int_0^{\infty} f(x) \, \mathrm{d}x + \sum_{k=1}^{\infty} d_k f^{(2k-1)}(0) h^{2k}, \qquad h \to 0 \tag{A 3}$$

for any function $f(x)$, regular for $x \geqslant 0$ and exponentially decaying with its derivatives at $x \to \infty$; universal coefficients d_k are connected to Bernoulli numbers B_{2k}. It is immediately seen from (A 3) that the terms with $(T_\alpha + T_\beta)$ represent regular contributions to (A 1)–(A 2) at $\epsilon \to 0$, expandable in integer power ϵ^k, $k \geqslant 0$. Singular sums in (A 1)–(A 2) can be regularized as

$$\sum_{n=0}^{\infty} \frac{\mathrm{e}^{-(n+1/2)\eta_0}}{\sinh(n+1/2)\eta_0} = \sum_{n=0}^{\infty} \mathrm{e}^{-(n+1/2)\eta_0} \left[\frac{1}{\sinh(n+1/2)\eta_0} - \frac{1}{(n+1/2)\eta_0} \right] + \frac{1}{\eta_0} \ln \coth(\tfrac{1}{4}\eta_0), \tag{A 4 a}$$

$$\sum_{n=0}^{\infty} \mathrm{e}^{-(2n+1)\eta_0} \coth(n + \tfrac{1}{2})\eta_0 = \frac{1}{\eta_0} \ln \coth(\tfrac{1}{2}\eta_0) + \sum_{n=0}^{\infty} \mathrm{e}^{-(2n+1)\eta_0} \left[\coth(n + \tfrac{1}{2})\eta_0 - \frac{1}{(n+1/2)\eta_0} \right] \tag{A 4 b}$$

and expanded using (A 3). Thus, the expressions (A 1)–(A 2) have the asymptotic structure $c_0 \ln \epsilon + c_1 + O(\epsilon \ln \epsilon)$ at $\epsilon \to 0$, as was stated in § 3, and the $O(\epsilon \ln \epsilon)$-terms come from the correction $\epsilon/6$ in the asymptotics $\sinh \eta_0/\eta_0 \sim 1 + \epsilon/6$. With the

original radius $a = \hat{a}(1 + \epsilon/2)$ instead of $\hat{a}$ in (A 1)–(A 2), the $O(\epsilon \ln \epsilon)$-terms would be 2 and 5 times larger, respectively. For this reason, the ratio $\hat{a}/a$, instead of unity, is used in (3.15) and (3.17).

To demonstrate that (3.14) can be a well-posed problem for all $\epsilon > 0$, we will show that the corresponding homogeneous problem for two spheres has only a zero solution. It follows from (A 1) and a similar expression for the flux through $\hat{S}_\beta$ that the boundary conditions (3.14) imply $T_\alpha + T_\beta = 0$ and are reduced to $\pi\hat{a}D(T_\alpha - T_\beta) = 0$, with

$$D(\epsilon) = 2\sinh\eta_0 \sum_{n=0}^{\infty} \frac{\mathrm{e}^{-(n+1/2)\eta_0}}{\sinh(n+1/2)\eta_0} + (1 + \tfrac{1}{2}\epsilon)\Psi_{\alpha\beta} - \ln\epsilon^{-1}. \tag{A 5}$$

When $\Psi_{\alpha\beta} > 0$, the function $D(\epsilon)$ attains its minimum value $\ln(\gamma^2/4) + H_\mathrm{c} + \Delta H_\mathrm{m}$ at $\epsilon \to 0$. Thus, $D(\epsilon) > 0$ for all $\epsilon > 0$, if $\gamma > 7.12$, and so $T_\alpha = T_\beta = 0$.

Appendix B. The expansion of a harmonic function into spherical harmonics

Lemma B 1. *Let $f(\boldsymbol{x})$ be a harmonic function, regular for $|\boldsymbol{x}| \leqslant R$. Then for $0 \leqslant \mu \leqslant \nu$*

$$\int_{|\boldsymbol{x}|=R} f(\boldsymbol{x}) Y_{\nu\mu}(\boldsymbol{x})\,\mathrm{d}\Omega = (2R)^\nu \left[\frac{4\pi}{(2\nu+1)!}\right]^{1/2} C_{\nu,\mu}(D_1 + \mathrm{i}D_2)^\mu D_3^{\nu-\mu} f(\boldsymbol{x})_{|\boldsymbol{x}=0}, \tag{B 1}$$

where $D_i = \partial/\partial x_i$ and the coefficients $C_{\nu,\mu}$ are defined by (5.12).

Proof. Green's theorem yields for $|\boldsymbol{x}| < R$

$$f(\boldsymbol{x}) = \frac{R^2}{4\pi} \int_{|\boldsymbol{y}|=R} \left[\frac{1}{|\boldsymbol{x}-\boldsymbol{y}|}\frac{\partial f}{\partial R}(\boldsymbol{y}) - f(\boldsymbol{y})\frac{\partial}{\partial R}\frac{1}{|\boldsymbol{x}-\boldsymbol{y}|}\right] \mathrm{d}\Omega_{\boldsymbol{y}}. \tag{B 2}$$

Applying the operator $(D_1 + \mathrm{i}D_2)^\mu D_3^{\nu-\mu}$ to both sides of (B 2), using Maxwell relation (Hobson 1955) in the form

$$\frac{Y_{\nu\mu}(\boldsymbol{x})}{|\boldsymbol{x}|^{\nu+1}} = (-2)^\nu \left[\frac{(2\nu+1)}{4\pi(2\nu)!}\right]^{1/2} C_{\nu\mu}(D_1 + \mathrm{i}D_2)^\mu D_3^{\nu-\mu}\left(\frac{1}{|\boldsymbol{x}|}\right) \tag{B 3}$$

and setting then $\boldsymbol{x} = 0$, we arrive at

$$2^\nu \left[\frac{(2\nu+1)}{4\pi(2\nu)!}\right]^{1/2} C_{\nu,\mu}(D_1 + \mathrm{i}D_2)^\mu D_3^{\nu-\mu} f(\boldsymbol{x})_{|\boldsymbol{x}=0}$$
$$= \frac{1}{4\pi R^{\nu-1}} \int_{|\boldsymbol{y}|=R} \left[Y_{\nu\mu}(\boldsymbol{y})\frac{\partial f}{\partial R}(\boldsymbol{y}) + \frac{(\nu+1)}{R} f(\boldsymbol{y}) Y_{\nu\mu}(\boldsymbol{y})\right] \mathrm{d}\Omega. \tag{B 4}$$

Using Green's theorem for the regular harmonic functions $|\boldsymbol{y}|^\nu Y_{\nu\mu}(\boldsymbol{y})$ and $f(\boldsymbol{y})$, we have

$$\int_{|\boldsymbol{y}|=R} Y_{\nu\mu}(\boldsymbol{y})\frac{\partial f}{\partial R}(\boldsymbol{y})\,\mathrm{d}\Omega = \frac{\nu}{R}\int_{|\boldsymbol{y}|=R} f(\boldsymbol{y}) Y_{\nu\mu}(\boldsymbol{y})\,\mathrm{d}\Omega, \tag{B 5}$$

and (B 1) follows from (B 4) and (B 5).

The relation (B 1) can be also obtained from a general integral theorem (Hobson 1955, § 103), but the present, self-contained derivation is much simpler. Obviously, the case $\mu < 0$ can be reduced to $\mu \geqslant 0$ by (5.7). ■

Appendix C. An absolutely stable scheme for calculating Wigner functions

According to the theory of Wigner functions (Biedenharn & Louck 1981; Nikiforov & Uvarov 1974), the rotational transformation of spherical harmonics $Y_{\ell m}(\theta,\phi)$ of a given order ℓ to a new coordinate system (θ',ϕ') is determined, to within trivial azimuthal rotations, by a complex orthogonal matrix $P^{\ell}_{mm'}(\psi)$ ($|m|$, $|m'| \leqslant \ell$), where ψ is the angle between the new and old x_3-axes (see also (24) of Zinchenko 1994*a*). The coefficients $P^{\ell}_{mm'}$ obey

$$P^{\ell}_{mm'} = P^{\ell}_{m'm}, \qquad P^{\ell}_{mm'} = P^{\ell}_{-m,-m'}, \tag{C 1}$$

so that only the case $|m'| \leqslant m \leqslant \ell$ has to be considered, and are related to Jacobi polynomials $P^{(\alpha,\beta)}_n(\cos\psi)$ (Nikiforov & Uvarov 1974; Biedenharn & Louck 1981). Real coefficients $Q^{\ell}_{mm'} = \mathrm{i}^{m-m'}P^{\ell}_{mm'}$ can be written for $|m'| \leqslant m \leqslant \ell$ as

$$Q^{\ell}_{mm'} = \frac{1}{2^m}\frac{C_{\ell,m'}}{C_{\ell,m}}(1-\eta)^{(m-m')/2}(1+\eta)^{(m+m')/2}P^{(m-m',m+m')}_{\ell-m}(\eta), \qquad \eta = \cos\psi. \tag{C 2}$$

In particular, explicit relations follow from (C 2):

$$Q^{\ell}_{\ell m'} = \left[\frac{(2\ell)!}{(\ell-m')!(\ell+m')!}\right]^{1/2}\left(\frac{1-\eta}{2}\right)^{(\ell-m')/2}\left(\frac{1+\eta}{2}\right)^{(\ell+m')/2}. \tag{C 3}$$

A recurrent scheme ($|m'| \leqslant m \leqslant \ell-1$)

$$Q^{\ell}_{mm'} = \left[\frac{(\ell+m)}{(\ell-m)(\ell^2-m'^2)}\right]^{1/2}(\ell\eta - m')Q^{\ell-1}_{mm'} - \left[\frac{(\ell-m-1)}{(\ell-m)(\ell^2-m'^2)}\right]^{1/2}\ell\sin\psi Q^{\ell-1}_{m+1,m'}, \tag{C 4}$$

which is derived from the relation between $\mathrm{d}P^{(\alpha,\beta)}_n(x)/\mathrm{d}x$, $P^{(\alpha,\beta)}_n(x)$ and $P^{(\alpha,\beta)}_{n+1}(x)$ (e.g. Abramowitz & Stegun 1964) and is equivalent to (27c) of Zinchenko (1994*a*), provides, in principle, the values of the rest Q–coefficients, but this method is numerically unstable for large ℓ (typically, for ℓ slightly above 100 in double precision calculations). An alternative scheme ($|m'|+1 \leqslant m \leqslant \ell$)

$$Q^{\ell}_{mm'} = \left[\frac{(\ell-m)}{(\ell+m)(\ell^2-m'^2)}\right]^{1/2}(\ell\eta + m')Q^{\ell-1}_{mm'} + \left[\frac{\ell+m-1}{(\ell+m)(\ell^2-m'^2)}\right]^{1/2}\ell\sin\psi Q^{\ell-1}_{m-1,m'} \tag{C 5}$$

derived from the relation between

$$P^{(\alpha,\beta)}_n(x), \qquad \frac{\mathrm{d}P^{(\alpha,\beta)}_n(x)}{\mathrm{d}x}, \qquad \frac{\mathrm{d}P^{(\alpha,\beta)}_{n+1}(x)}{\mathrm{d}x}$$

would be stable, but provides no way of calculating $Q^{\ell}_{m,\pm m}$. Instead, a recurrent relation ($|m'|+1 \leqslant m \leqslant \ell$)

$$Q^{\ell}_{m-1,m'} + \frac{2(m'-\eta m)}{\sin\psi[(\ell+m)(\ell-m+1)]^{1/2}} Q^{\ell}_{mm'} + \left[\frac{(\ell+m+1)(\ell-m)}{(\ell+m)(\ell-m+1)}\right]^{1/2} Q^{\ell}_{m+1,m'} = 0 \quad (C\,6)$$

(with the last term set to zero for $m = \ell$) can be derived from (C 4) and (C 5). Starting from (C 3), all the coefficients $Q^{\ell}_{mm'}$ with $m = \ell-1, \ell-2, \ldots, |m'|$ can be found successively from (C 6). We used this scheme to calculate rotational matrices for random particle configurations and $\ell \leqslant 550$, and found the exact relation

$$\sum_{|m'|\leqslant\ell} |P^{\ell}_{mm'}|^2 = 1 \quad (C\,7)$$

to hold at least to $O(10^{-13})$, which suggests the numerical stability of this scheme for all ℓ. With square roots in (C 6) factorized and calculated beforehand, this scheme is almost as economical as that of Zinchenko (1994*a*).

References

Abramowitz, M. & Stegun, I. A. 1964 *Handbook of mathematical functions*. NBS Applied Mathematics Series, vol. 55. Paris: Flammarion.

Bagi, K. 1993 A quasi-static numerical model for micro-level analysis of granular assemblies. *Mech. Mater.* **16**, 101.

Barbosa, R. E. & Ghaboussi, J. 1990 Discrete finite element method for multiple deformable bodies. *Finite Elem. Analysis Design* **7**, 145.

Barbosa, R. & Ghaboussi, J. 1992 Discrete finite element method. *Engng Comput.* **9**, 253.

Batchelor, G. K. & O'Brien, R. W. 1977 Thermal or electrical conduction through a granular material. *Proc. R. Soc. Lond.* A **355**, 313.

Bateman, H. & Erdelyi, A. 1953 *Higher transcendental functions*. New York: McGraw-Hill.

Biedenharn, L. C. & Louck, J. D. 1981 *Angular momentum in quantum physics: theory and application*. Reading, MA: Addison-Wesley.

Bonnecaze, R. T. & Brady, J. F. 1990 A method for determining the effective conductivity of dispersions of particles. *Proc. R. Soc. Lond.* A **430**, 285.

Bonnecaze, R. T. & Brady, J. F. 1991 The effective conductivity of random suspensions of spherical particles. *Proc. R. Soc. Lond.* A **432**, 445.

Bojtár, I. & Bagi, K. 1993 Numerical analysis of loose and bonded granular materials. *Mech. Mater.* **16**, 111.

Bossis, G. & Brady, J. F. 1984 Dynamic simulation of sheared suspensions. I. General method. *J. Chem. Phys.* **80**, 5141.

Brady, J. F. & Bossis, G. 1985 The rheology of concentrated suspensions of spheres in simple shear flow by numerical simulation. *J. Fluid Mech.* **155**, 105.

Chan, C. K. & Tien, C. L. 1973 Conductance of packed spheres in vacuum. *ASME J. Heat Transfer* **95**, 302.

Cooley, M. D. A. & O'Neill, M. E. 1969 On the slow motion generated in a viscous fluid by the approach of a sphere to a plane wall or stationary sphere. *Mathematika* **16**, 37.

Cundall, P. A. & Strack, O. D. L. 1979 A discrete numerical model for granular assemblies. *Géotechnique* **29**, 47.

Davis, R. H., Serayssol, J. & Hinch, E. J. 1986 The elastohydrodynamic collision of two spheres. *J. Fluid Mech.* **163**, 479.

Dobry, R. & Ng, T. 1992 Discrete modelling of stress–strain behaviour of granular media at small and large strains. *Engng Comput.* **9**, 129.

Duncan, A. B., Peterson, G. P. & Fletcher, L. S. 1989 Effective thermal conductivity within packed beds of spherical particles. *ASME J. Heat Transfer* **111**, 830.

Goddard, J. D., Zhuang, X. & Didwania, A. K. 1993 Microcell methods and the adjacency matrix in the simulation of the mechanics of granular media. In *Proc. 2nd Int. Conf. on Discrete Element Methods* (ed. J. R. Williams & G. G. W. Mustoe), pp. 3–14. MIT, Cambridge, MA: ISEL Publ.

Goddard, J. D., Didwania, A. K. & Zhuang, X. 1994 Computer simulations and experiment on the quasi-static mechanics and transport properties of granular materials. In *Mobile particulate systems* (ed. E. Guazzelli & L. Oger), pp. 261–280. Dordrecht: Kluwer.

Hobson, E. W. 1955 *The theory of spherical and ellipsoidal harmonics.* New York: Chelsea.

Jodrey, W. S. & Tory, E. M. 1981 Computer simulation of isotropic, homogeneous, dense random packing of equal spheres. *Powder Technol.* **30**, 111.

Jodrey, W. S. & Tory, E. M. 1985 Computer simulation of close random packing of equal spheres. *Phys. Rev.* A **32**, 2347.

Kim, I. C. & Torquato, S. 1991 Effective conductivity of suspensions of hard spheres by Brownian motion simulation. *J. Appl. Phys.* **69**, 2280.

Kim, I. C. & Torquato, S. 1992 Effective conductivity of suspensions of overlapping spheres. *J. Appl. Phys.* **71**, 2727.

Kim, I. C. & Torquato, S. 1993 Effective conductivity of composites containing spheroidal inclusions: comparison of simulations with theory. *J. Appl. Phys.* **74**, 1844.

Kling, G. 1938 Das warmeleitvermögen eines Kugelhaufwerks in ruhenden. *Gas. Forsch. Geb. Ingeniew* **9**, 28.

Landau, L. D. & Lifshitz, E. M. 1959 *Theory of elasticity.* New York: Pergamon Press.

McKenzie, D. R., McPhedran, R. C. & Derrick, G. H. 1978 The conductivity of lattices of spheres. II. The body-centered and face-centered cubic lattices. *Proc. R. Soc. Lond.* A **362**, 211.

McPhedran, R. C. & McKenzie, D. R. 1978 The conductivity of lattices of spheres. I. The simple cubic lattice. *Proc. R. Soc. Lond.* A **359**, 45.

McWaid, T. & Marschall, E. 1992 Thermal contact resistance across pressed metal contacts in a vacuum environment. *Int. J. Heat Mass Transfer* **35**, 2911.

Mindlin, R. D. & Deresiewicz, H. 1953 Elastic spheres in contact under varying oblique forces. *ASME J. Appl. Mech.* **20**, 327.

Morse, P. & Feshbach, H. 1953 *Methods of theoretical physics.* New York: McGraw-Hill.

Moscinski, J., Bargiel, M., Rycerz, Z. A. & Jacobs, P. W. M. 1989 The force-biased algorithm for the irregular close packing of equal hard spheres. *Mol. Simul.* **3**, 201.

Mullier, M., Tüzün, U. & Walton, O. R. 1991 A single-particle friction cell for measuring contact frictional properties of granular materials. *Powder Technol.* **65**, 61.

Nakajima, K. 1995 Thermal contact resistance between balls and rings of a bearing under axial, radial, and combined loads. *J. Thermophys. Heat Transfer* **9**, 88.

Negus, K. J., Yovanovich, M. M. & Thompson, J. C. 1987 Constriction resistance of circular contacts on coated surfaces: effect of boundary conditions. *J. Thermophys.* **2**, 158.

Nikiforov, A. F. & Uvarov, V. B. 1974 *The foundations of special function theory.* Moscow: Nauka. (In Russian.)

Onoda, G. & Liniger, E. G. 1990 Random loose packings of uniform spheres and the dilatancy onset. *Phys. Rev. Lett.* **64**, 2727.

Sangani, A. & Mo, G. 1994 Inclusion of lubrication forces in dynamic simulations. *Phys. Fluids* **6**, 1653.

PHILOSOPHICAL TRANSACTIONS OF THE ROYAL SOCIETY A MATHEMATICAL, PHYSICAL & ENGINEERING SCIENCES

Sangani, A. S. & Yao C. 1988 Bulk thermal conductivity of composites with spherical inclusions. *J. Appl. Phys.* **63**, 1334.

Scott, G. D. & Kilgour, D. M. 1969 The density of random close packing of spheres. *Brit. J. Appl. Phys. Ser. 2* **2**, 863.

Song, S. & Yovanovich, M. M. 1988 Relative contact pressure: dependence on surface roughness and Vickers microhardness. *J. Thermophys.* **2**, 43.

Song, S., Yovanovich, M. M. & Nho, K. 1989 Thermal gap conductance: effects of gas pressure and mechanical load. *J. Thermophys.* **6**, 62.

Song, S., Yovanovich, M. M. & Goodman, F. O. 1993 Thermal gap conductance of conforming surfaces in contact. *ASME J. Heat Transfer* **115**, 533.

Sridhar, M. R. & Yovanovich, M. M. 1994 Review of elastic and plastic contact conductance models: comparison with experiment. *J. Thermophys. Heat Transfer* **8**, 633.

Turner, J. C. R. 1973 Electrical conductivity of liquid-fluidized beds. *Am. Inst. Chem. Engng Symp. Series* **69**, 115.

Woodcock, L. V. 1976 Glass transition in the hard-sphere model. *J. Chem. Soc., Faraday Trans. II* **72**, 1667.

Yiantsios, S. G. & Davis, R. H. 1990 On the buoyancy-driven motion of a drop towards a rigid surface or a deformable interface. *J. Fluid Mech.* **217**, 547.

Yiantsios, S. G. & Davis, R. H. 1991 Close approach and deformation of two viscous drops due to gravity and van der Waals forces. *J. Colloid Interface Sci.* **144**, 412.

Yovanovich, M. M. 1975 Thermal constriction resistance of contacts on a half-space: integral formulation. AIAA paper 75–708.

Zhang, Y. & Cundall, P. A. 1986 Numerical simulation of slow deformations. In *Proc. Symp. Mech. Particulate Media, Tenth US Nat. Congr. Appl. Mech., University of Texas, Austin.*

Zinchenko, A. Z. 1994*a* An efficient algorithm for calculating multiparticle thermal interaction in a concentrated dispersion of spheres. *J. Comput. Phys.* **111**, 120.

Zinchenko, A. Z. 1994*b* Algorithm for random close packing of spheres with periodic boundary conditions. *J. Comput. Phys.* **114**, 298.